2008-01-01

A Novel Series of Viologen-Containing Dendrimers

Papri Bhattacharya
University of Miami, p.bhattacharya@umiami.edu

UNIVERSITY OF MIAMI

A NOVEL SERIES OF VIOLOGEN-CONTAINING DENDRIMERS

By

Papri Bhattacharya

A THESIS

Submitted to the Faculty
of the University of Miami
in partial fulfillment of the requirements for
the degree of Master of Science

Coral Gables, Florida

May 2008

UNIVERSITY OF MIAMI

A thesis submitted in partial fulfillment of
the requirements for the degree of
Master of Science

A NOVEL SERIES OF VIOLOGEN-CONTAINING DENDRIMERS

Papri Bhattacharya

Approved:

_____ Dr. Angel E. Kaifer Professor of Chemistry	_____ Dr. Terri A. Scandura Dean of the Graduate School
_____ Dr. Roger M. Leblanc Professor of Chemistry	_____ Dr. Thomas K. Harris Assistant Professor of Chemistry
_____ Dr. Richard S. Myers Lecturer of Biochemistry & Molecular Biology	

Bhattacharya, Papri (M.S., Chemistry)

A Novel Series of Viologen-Containing Dendrimers (May 2008)

Abstract of a thesis at the University of Miami.

Thesis supervised by Professor Angel E. Kaifer.

No. of pages in text: (56)

This dissertation investigates the synthesis, characterization and electrochemical properties of viologen-containing dendrimers. Additionally, the self-assembled system of resorcinarenes was investigated with paramagnetic guests using EPR and ^{1}H NMR techniques.

Chapter one is a brief introduction to the dendrimers and describes its evolution, structural features, synthetic methods and emerging applications to various fields of research such as catalysis, material science, drug delivery and medicine.

Chapter two describes the synthesis, characterization and electrochemical properties of a new series of dendrimers. These dendrimers have a viologen unit at the core surrounded by Newkome and Fréchet dendrons. The potentials of two consecutive one-electron reductions of the viologen core were determined by cyclic voltammetry. The electrochemistry of viologen unit showed a distinct and obvious trend. Newkome and Fréchet dendrons having different functional groups as repeating units has opposite effect on the half-wave potentials. The overall effect of these two dendrons is reflected by the corresponding reduction

potentials. The redox site encapsulation by the Fréchet and Newkome dendrons is indicated by the attenuation in heterogeneous electron transfer rate constants.

Chapter three describes the probing of self-assembled capsule of resorcinarenes with 4-amino tempo and 4-trimethyl-ammonium tempo derivative. EPR spectroscopy and ^{1}H NMR spectroscopy were used to investigate the nature of complexations involved in these systems. We observed a subsequent change in their spectroscopic parameters. Careful investigation of rotational correlation times and NMR line-widths at half height revealed that 4-trimethyl-ammonium tempo has stronger binding affinity with these capsules compared to 4-amino tempo due to favorable cation $-\pi$ interactions.

TABLE OF CONTENTS

LIST OF FIGURES

LIST OF TABLES

Chapter II Page

LIST OF SCHEMES

LIST OF SPECTRA

Chapter I

INTRODUCTION TO DENDRIMERS: STRUCTURE, PROPERTIES AND APPLICATIONS

1.1 Background and History

The word "dendrimer" comes from the Greek dendrons, meaning trees, and meros, meaning part. We may imagine a tree in which each of its branches divides into new branches after a certain length. This continues repeatedly until the branches become so densely packed that the canopy forms a globe. In a dendrimer, repeating branching units or dendrons converge to a single focal point or core. Dendrimers are highly branched, monodisperse, tree-shaped macromolecules.[1] Initially, they got attention due to the special molecular architecture, very soon it was realized that they can be very useful and could have diverse applications. They are a special class of polymeric materials, very different from traditional polymers. Traditional polymers are made from AB monomers while dendrimers are made of AB_n (n= 2, 3) type of monomers. Another significant difference between traditional polymers and dendrimers is that dendrimers have a well-defined molecular weight while traditional polymers do not.[2]

The chemistry of dendrimers first started in 1978 when Vögtle and coworkers published the synthesis of the first dendrimer.[3] In 1979, Denkewalter *et al.* filed a patent on branched macromolecules with amino acid as the repeating unit.[4] Subsequently, Donald A. Tomalia *et al.*[5] developed the industrial preparation of polyamidoamine (PAMAM) (**Figure 1.1**) and took dendrimer

chemistry to a new level, opening a new area of science. The fascinating structure and the unique properties of these molecules attracted many research groups.[6-9] Very soon, dendrimer chemistry started growing into many interesting dimensions.

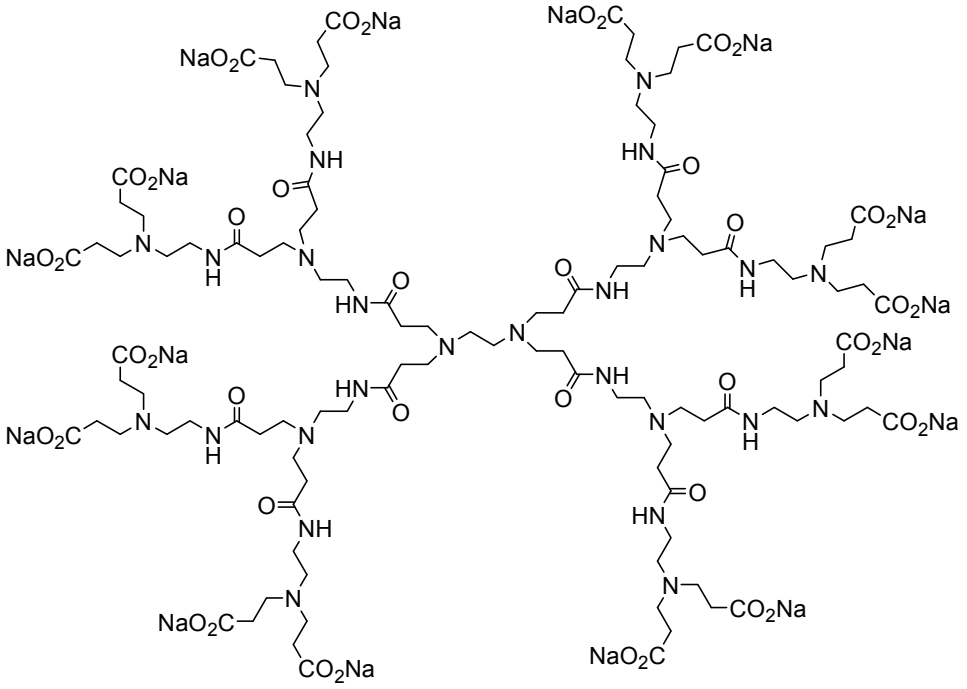

Figure 1.1 *Polyamidoamine dendrimer containing carboxylate groups on its external surface.*

1.2 General Molecular Architecture of Dendrimers

Dendrimers at lower generations (G) have a floppy, disk like structure. At higher generations (generally G>4) where the number of branches increases, dendrimers adopt a globular structure. Generally, the branches or "dendrons" start coming outwards from a "core". Near the core, there are empty spaces or "internal cavities"[10] and, near the periphery, the branches are closely packed (**Figure 1.2**). After a certain generation number, the peripheral groups are so

closely packed that the dendrimer's growth stops. This is called the 'starburst effect'.[11] For example, for PAMAM dendrimer synthesis it is observed after the tenth generation.

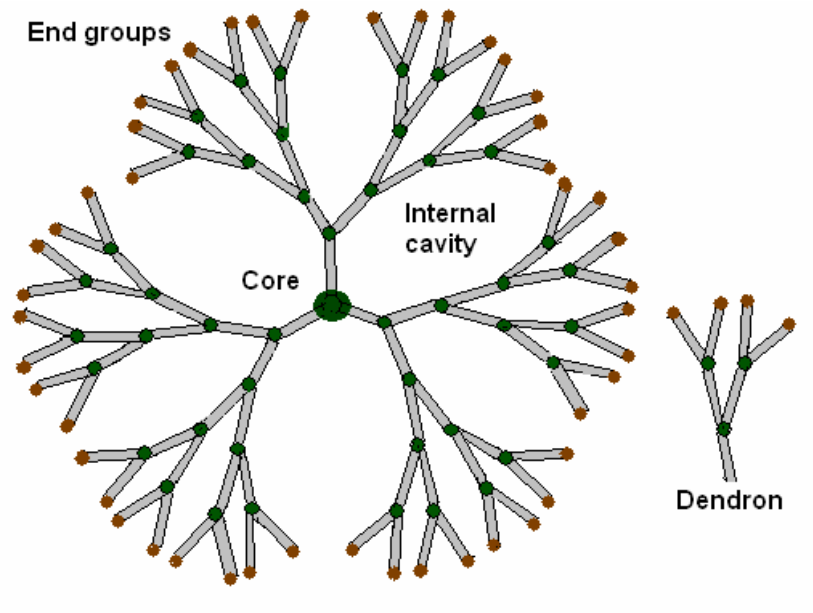

Fig 1.2 *General structure of a dendrimer*

Functionalization of dendrimers can be done at their cores or in the branching units or on the periphery. For example, the terminal groups can be functionalized with positively charged groups and thus the dendrimer will act like a polyelectrolyte. In addition, the "internal cavities" are capable of trapping molecules and may be exploited in supramolecular chemistry. These internal cavities or voids are not very rigid but are capable of changing shape and conformation to allow intermolecular encapsulation.[12]

1.3 Synthesis of Dendritic Structures

Synthesis of dendrimers requires a fully controlled, step-by-step approach. Two main synthetic strategies for synthesizing dendrimers have emerged over the past decade: the divergent and convergent approaches.

1.3.1 Divergent Approach

In the divergent strategy, pioneered by Newkome and Tomalia, the dendrimer is built out from a core, layer by layer. At each growing step, a new layer of branching units is added, thus increasing the generation number by one.[13] The core molecule reacts with monomer molecules containing one reactive and two dormant groups to give the first generation dendrimer. The new periphery of the molecule is activated for reactions with more monomers in each repeat cycle. The periphery reacts with monomer units to add a new layer or generation to the dendrimer. In the next repeat cycle, two or three times as many reactive sites will be available depending on whether the monomer unit's branch multiplicity is 2 or 3 (i.e., AB_2 vs. AB_3 monomer). This process is repeated until required degree of branching is obtained. Although the divergent synthesis has many good features, it requires the growing dendrimers to undergo tens and even hundreds of reactions simultaneously. This can lead to a mixture of dendrimers with similar structures rather than a uniform final product.

Unlike traditional polymers, synthesis of dendrimers requires very efficient reactions to avoid flaws in the dendrimer structure, because increasing generations exponentially increases number of reactions that must take place

simultaneously. Classical example of divergent methods is the dendrimer synthesis by Vögtle and coworkers (**Figure1.3**). Each layer of branching is added only after the nitrile groups are reduced to amine functionalities. In this way, the reaction is fully controlled and the dendrimer is built from the core outwards the periphery.

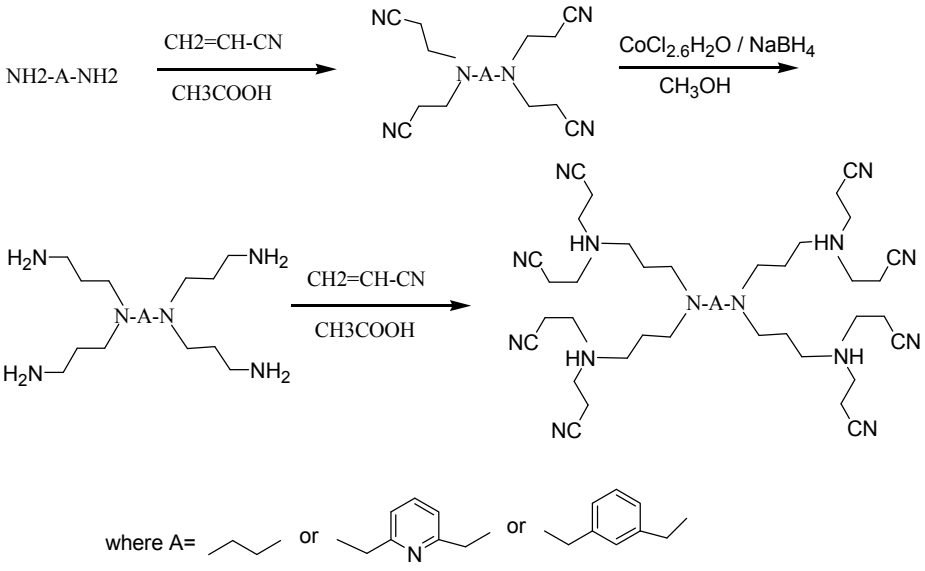

Figure1.3 *Synthesis of polyamine dendrimers by Vögtle and coworkers.*

1.3.2 Convergent Approach

In the convergent approach, the dendrimer is constructed step by step, starting from the end groups and progressing inwards. First the dendrons are synthesized and when the desired generation number is achieved, they are attached to a core.

Hawker and Fréchet pioneered the convergent approach[14] to overcome the problems associated with the divergent synthesis. The convergent method is

more advantageous over the divergent method. In convergent method, there are less number of reactions, generally 2-3, taking place in each step. On the other hand, the divergent approach comprises numerous reactions. Sometimes hundreds of reactions must take place in a single step. Therefore, dendrimers are less prone to defects in the dendritic structure when it is synthesized by convergent approach.

1.4 Applications

The special molecular architecture of dendrimers gives rise to the possibility of being used in various technological applications. By tuning the functional groups in the periphery, the core or the interior, the properties, size and shape of dendrimers can be designed to serve many applications in fields like catalysis, drug delivery and tissue engineering.

1.4.1 Dendritic Sensors

The periphery of dendrimers can be functionalized with appropriate functional groups enabling them to act as sensors. Balzani *et al*.[15] have functionalized the peripheral groups of a PAMAM dendrimer with 32 dansyl units. The interior of this dendrimer has 30 aliphatic amine units that are capable of coordinating with suitable metal ions (**Figure 1.4**). They have shown that when a Co^{2+} ion was incorporated, the strong fluorescence of the dansyl groups was quenched. The presence of many fluorescent groups at the periphery of the dendrimer makes it an effective sensor for Co^{2+}.

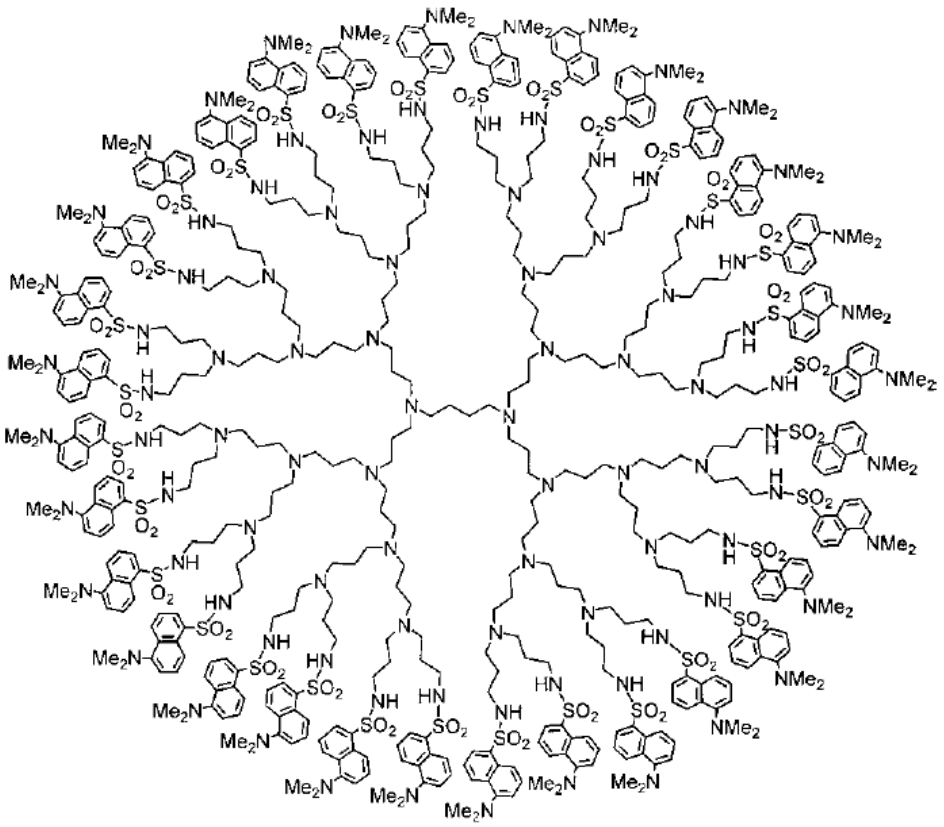

Figure 1.4 *PAMAM dendrimer with 32 dansyl groups on the periphery.*[15]

1.4.2 Catalysis

Dendrimers may be functionalized to work as catalysts with excellent specificity and high efficiency. When the peripheral functional groups of a dendrimer are replaced by catalytic sites, a single molecule of dendrimer can work as a highly efficient polyvalent catalyst. One of the advantages of this kind of dendritic catalyst is that, with appropriate peripheral functional groups, they can work as a homogeneous catalyst. After the reaction is completed, the dendritic catalyst can be separated very easily by nanofiltration.

One of the examples of the dendritic catalyst was prepared by Hoveyda and co-workers[16] based on ruthenium (**Figure 1.5**).

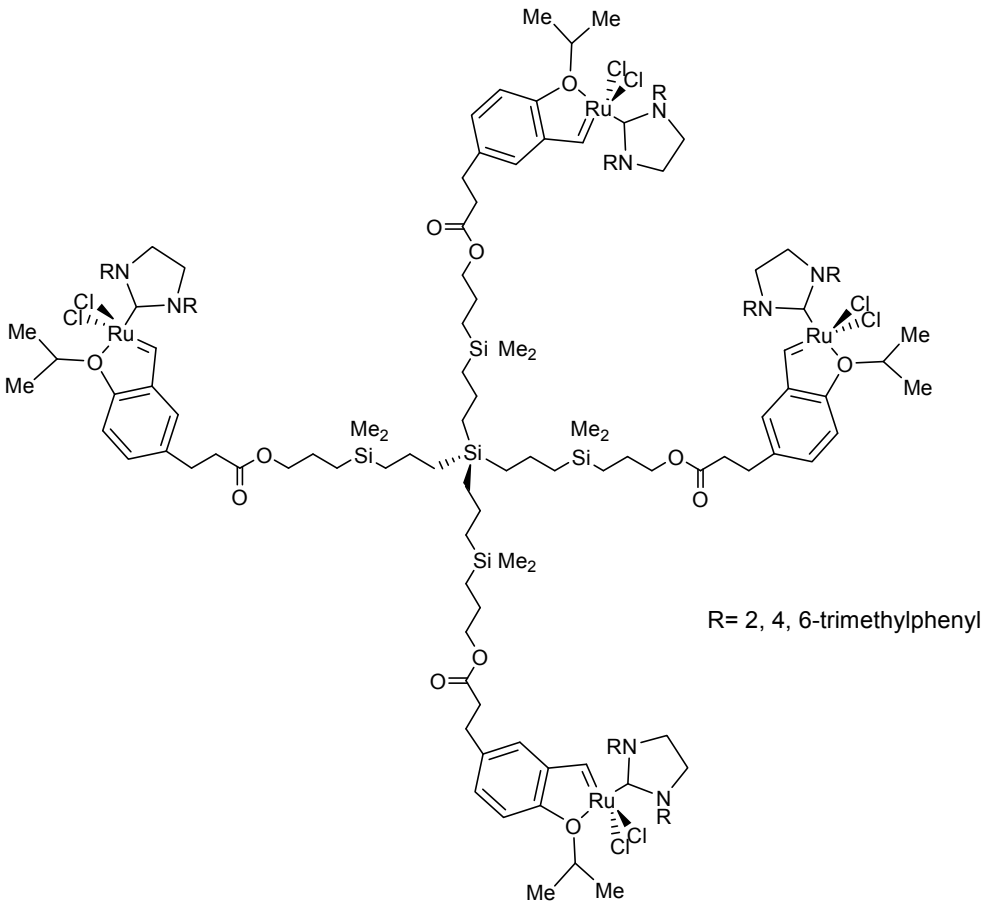

Figure 1.5 *Ruthenium containing catalytic dendrimer for metathesis reaction.*

1.4.3 Biological Applications

Recently there have been several attempts to use dendrimers in biological applications, although the toxicity of dendritic materials has been the main concern for the actual application to mankind.

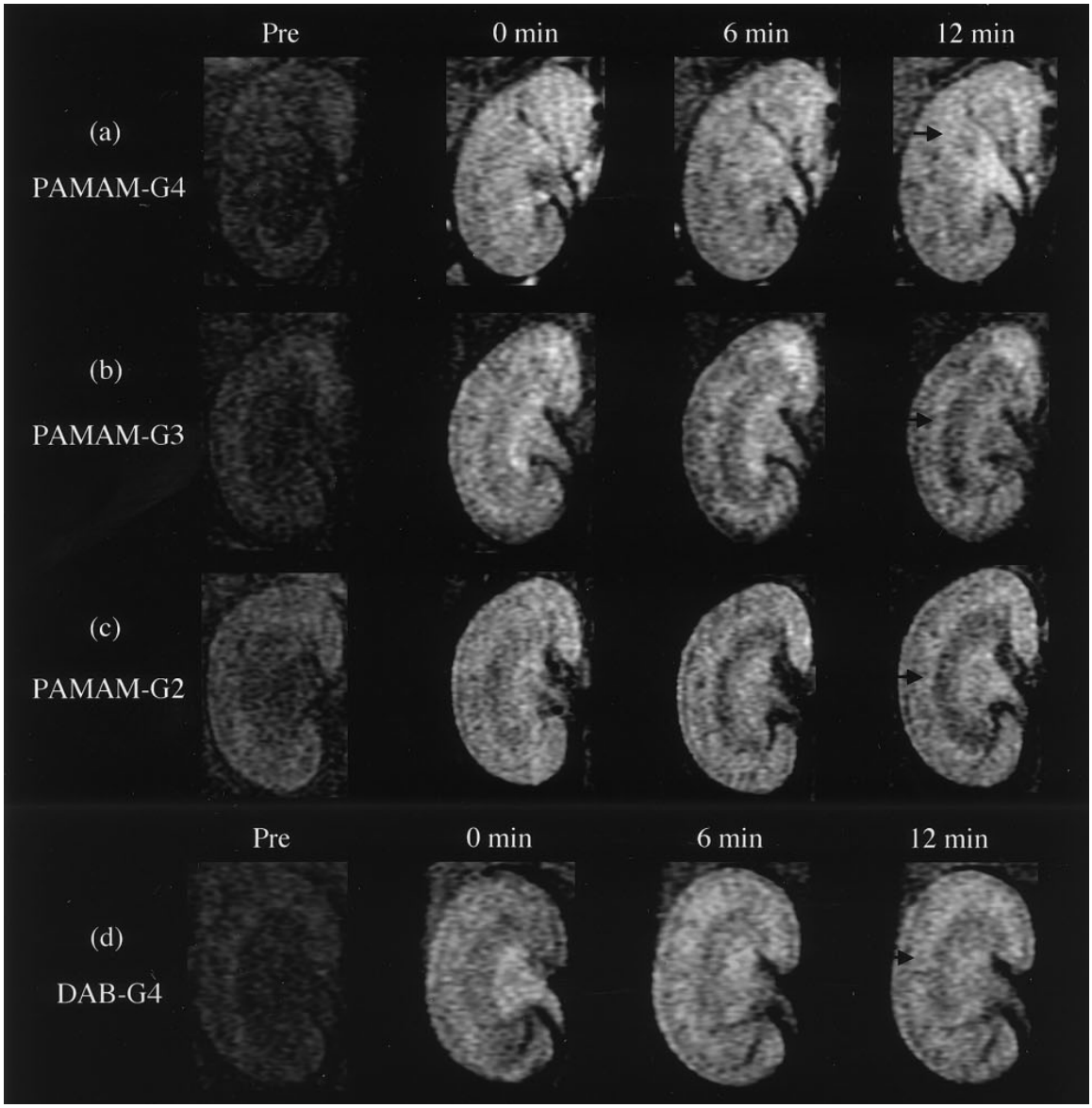

Figure 1.6 *Coronal high-resolution images of contrast enhanced dynamic micro-MRI at the center of the right kidney obtained preinjection, or 0, 6, and 12 minutes postinjection of 0.03 mmol/kg of contrast agent: PAMAM-G4 (**a**), PAMAM-G3 (**b**), PAMAMG2 (**c**), DAB-G4 (**d**), DAB-G3.* [18]

Encapsulation of guest molecules in the void or cavity of dendrimers can be used to deliver therapeutic agents throughout the body. For example, Dendritic Nanotechnologies uses the voids in a polyamidoamine dendrimer to host cis-

platin or carboplatin anticancer drugs.[17] Dendrimers have also been used in molecular imaging technology. For example, polypropylenimine diaminobutyl (DAB) and PAMAM dendrimers were used as MRI contrast agents and have shown high efficiency (**Figure 1.6**).[18]

1.5 Conclusion and Outlook

Dendrimers are aesthetically appealing macromolecules with high potential. Although the chemistry of dendrimers started evolving recently, it has grown exponentially with time, which is reflected by the number of published papers, books and articles. At the beginning, the main concern in this area of research was directed towards the development of new synthetic routes. Presently there are many synthetic routes available and even some of the dendrimers are available commercially. Recent trends in dendrimer chemistry are focused on finding new potential applications benefitting from its structural features and properties. Being a macromolecule with a nanometer scale size and wide variety of functionalities, the potential applications are diverse ranging from nanotechnology, medicine, tissue engineering to polymer science.

Chapter II

A NOVEL SERIES OF VIOLOGEN-CONTAINING DENDRIMERS

2.1 Redox-Active Dendrimers

Very important work on dendrimers is focused on their functionalization. Functionalization of dendrimers is the most important aspect to investigate its potential applications in various fields. Initially scientists were attracted to its aesthetic molecular architecture, but advancement in synthetic strategies allowed various changes in functionalities of predetermined sites of the molecule to perform various tasks at the molecular level. Their nanometer scale size and precise structure have attracted considerable amount of interest from biological and nanotechnological point of view.[2]

Our group is particularly interested in functionalization of dendrimers with redox active groups. The functionalization can be done in two ways: at the core or at the periphery. One of the classical examples of periphery-functionalized dendrimer is the 32-ferrocene dendrimer (**Figure 2.1**).[19] One of the interesting features of this dendrimer is that, all 32 ferrocene residues undergo oxidation reversibly at the same potential.

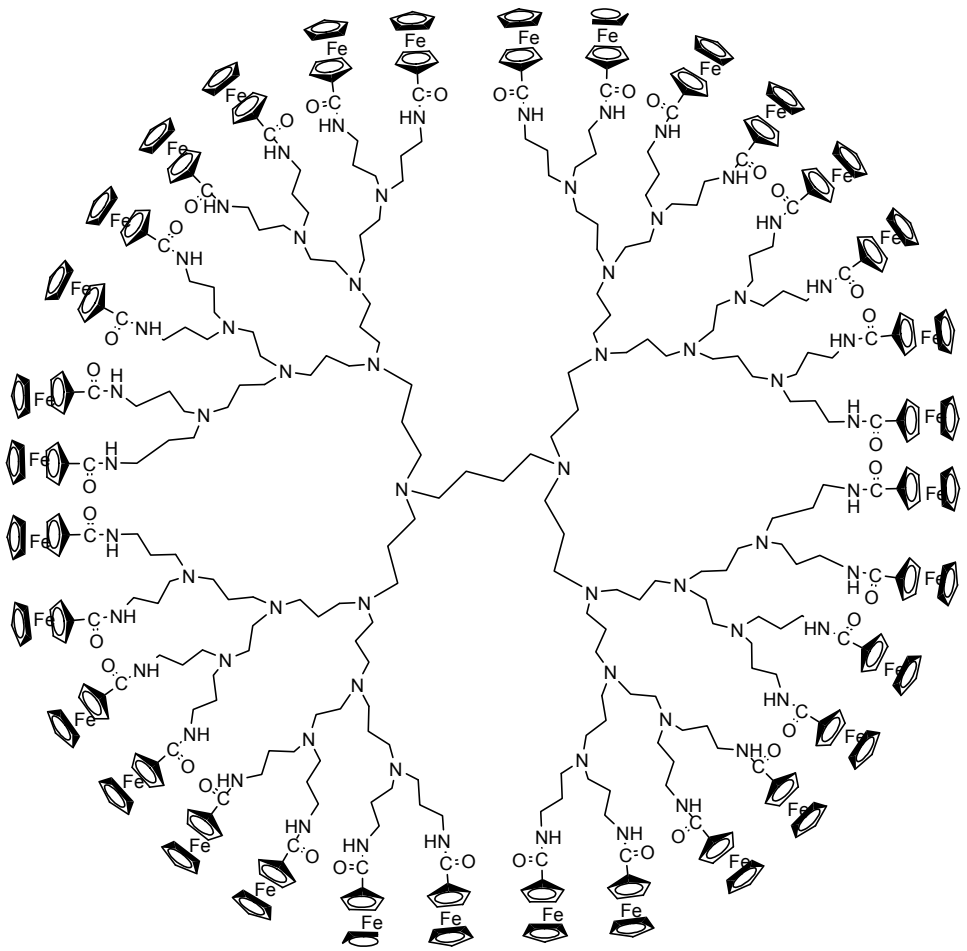

Figure 2.1 *Redox dendrimer with 32 ferrocene residue on the periphery.*

Our group has worked on both periphery functionalized and core functionalized dendrimers in the past. For example, we studied the electrochemical behavior of Newkome dendrimers with a ferrocene core (**Figure 2.2**). In less polar solvents, the Newkome dendron creates a polar microenvironment around the ferrocene core that favors the formation of the positive charge: in other words, with increasing generation number of Newkome dendron, the oxidation of the ferrocene residue happens at lower potential.[20]

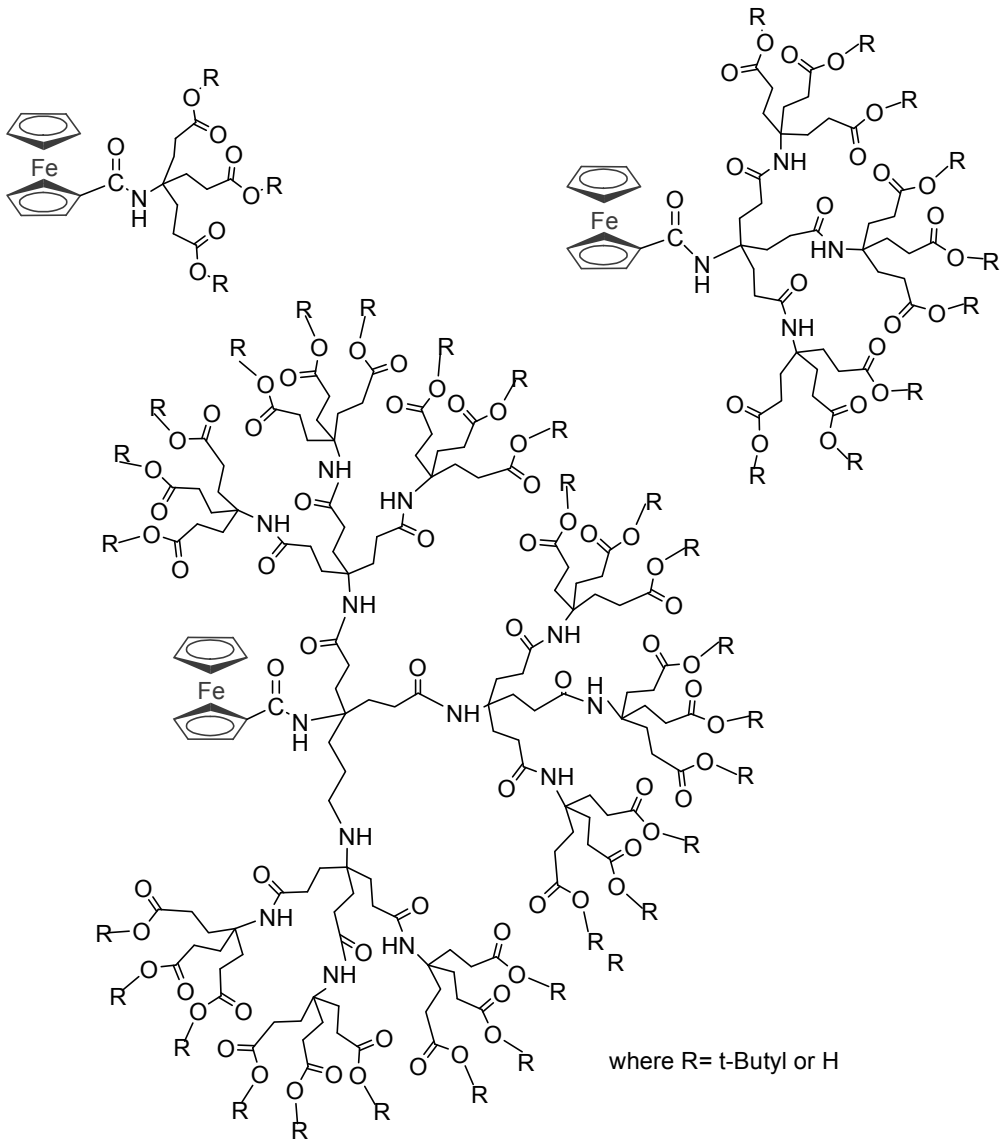

Figure 2.2 *Newkome type dendrons with ferrocene residue at the core.*

These redox active dendrimers can be compared with redox proteins[21] by both size and function. Similar to the redox proteins, the redox centers of these dendrimers are partially or fully buried in the dendritic branches. The electrochemical parameters show significant difference with increasing generation number of the dendron. In addition, the rate of heterogeneous electron transfer decreases as the size of the dendrimer increases.

My current research is focused on the design and synthesis of novel dendrimers containing a “viologen unit” at the core. In the past, our group had studied viologen-containing Fréchet and Newkome type dendrimers.[21] The main idea of my present work is to attach a Fréchet dendron and a Newkome dendron to a viologen core and study the effect of these two different kind of dendrons on the electrochemical behavior of the viologen moiety. The viologen core will give rise to interesting electrochemical properties in this kind of dendrimers. The 4,4'-bipyridinium unit, often called viologen (V^{2+}), is well known for its electron-accepting properties. Its electrochemical behavior is characterized by two reversible reduction waves, corresponding to the formation of a cation radical ($V^{+\bullet}$) and a neutral species (V), respectively.

2.2 Synthesis

The Newkome type building blocks N1E, N2E and N3E were synthesized according to convergent approach following published the methods.[22] Similarly, the Fréchet building blocks F1, F2 and F3 were also synthesized by convergent approach according to the original synthetic route reported by Fréchet and Hawker.[7]

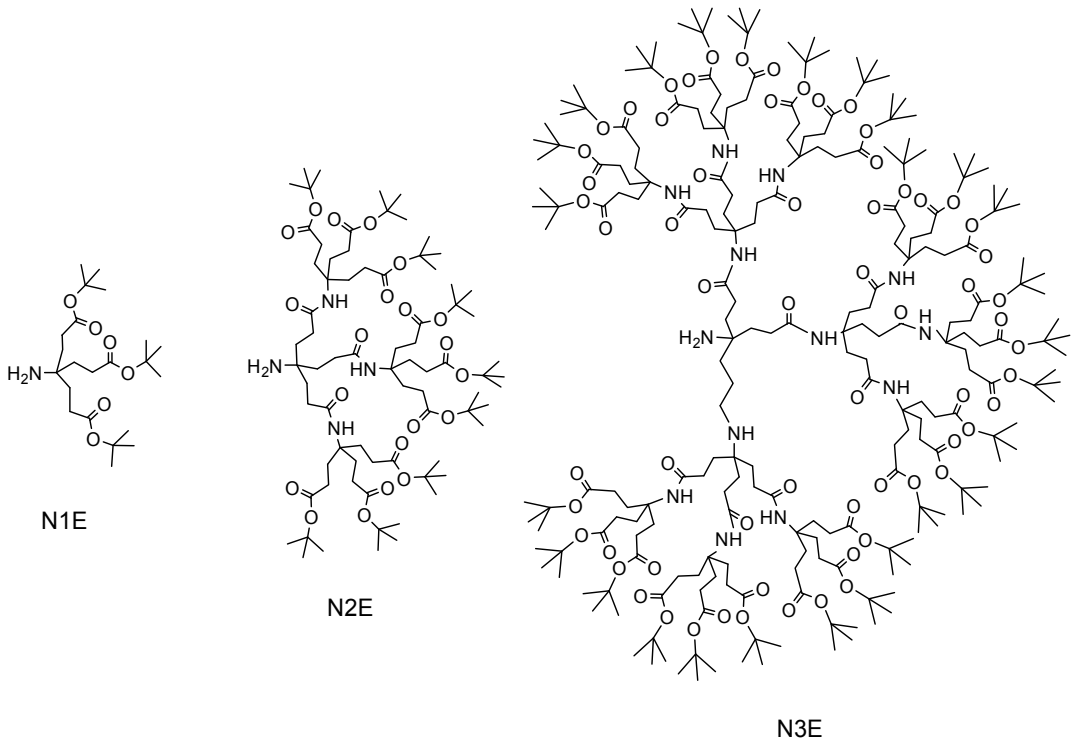

Figure 2.3 *The Newkome dendron building blocks: N1E, N2E, N3E represent the 1st, 2nd and 3rd generation of the Newkome dendron with ester terminal group.*

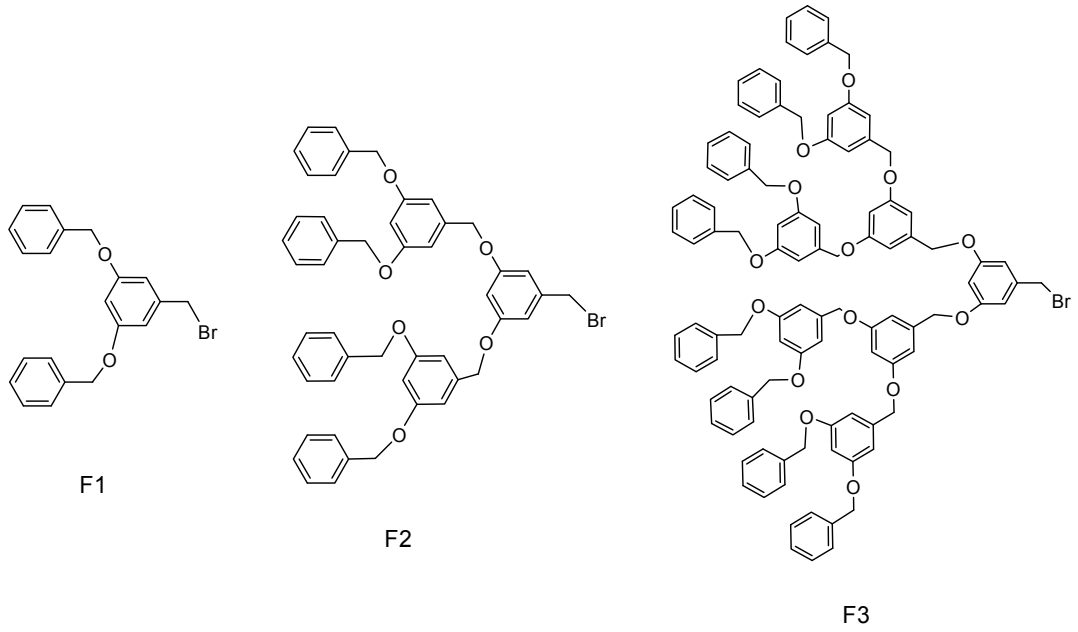

Figure 2.4 *The Fréchet dendron building blocks: F1, F2, F3 represent 1st, 2nd and 3rd generation of the Fréchet dendron*.

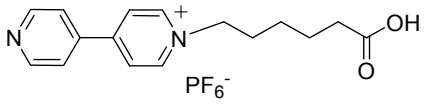

Figure 2.5 *Viologen core (V).*

The Fréchet dendron was then attached to the viologen moiety according to the known method from our lab.[21] The acid group on the viologen moiety was then coupled with the amine group of the Newkome dendron using HATU. The overall synthetic scheme is illustrated below for the hybrid dendrimers with both first generation of the Fréchet and the Newkome dendrons.

Synthetic Scheme 2.1

Step1:

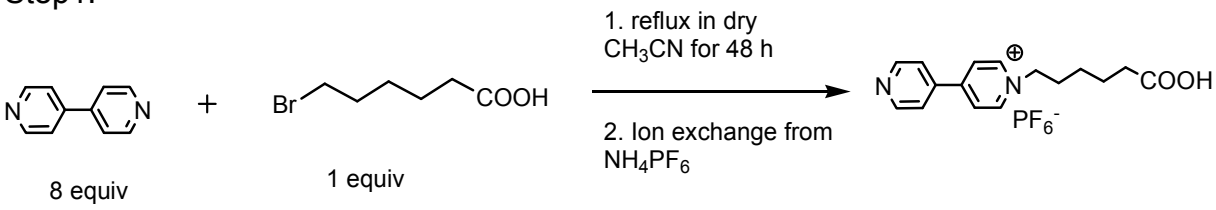

Step 2:

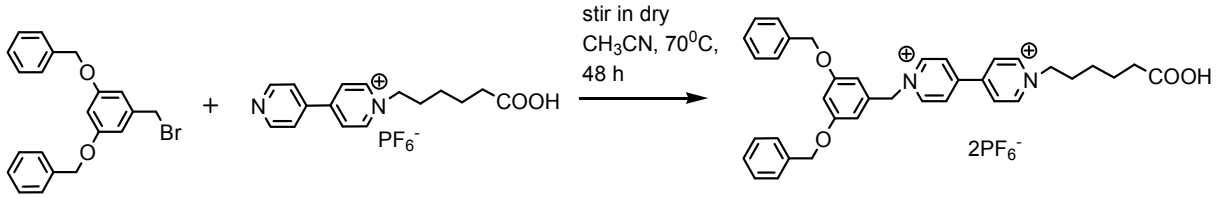

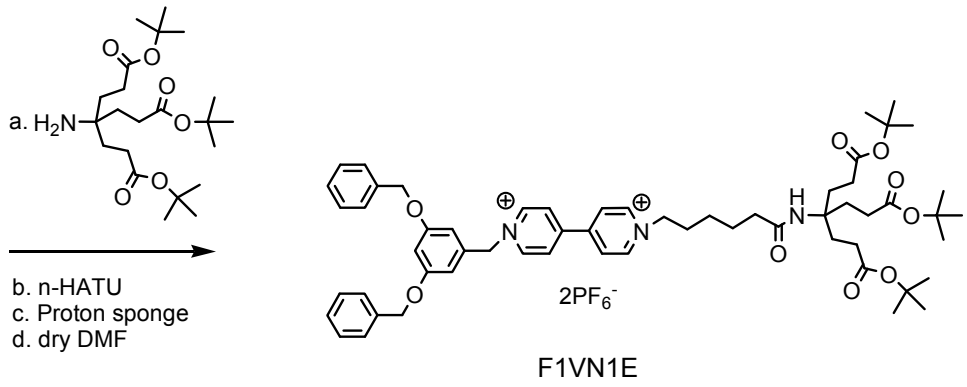

F1VN1E

Following the same procedure, all other hybrid dendrimers were synthesized but the Fréchet and the Newkome dendrons used were varied in Step 3 to get the desired hybrid dendrimer.

The viologen group at the dendrimer core is shielded by the Newkome and Fréchet dendrons. This gives rise to structures with partially or completely buried redox centers, which may resemble redox proteins. In addition, the heterogeneous electron transfer properties of viologen core may slow down when it is surrounded by two dendrons. This is in agreement with the natural process that happens in redox proteins where electron transfer process of the metal center, situated in the center or off- center of a huge polypeptide chain, shows significant orientation effect and slower rate of electron transfer.[23]

The structures of the novel viologen core dendrimers synthesized for my present work are given below:

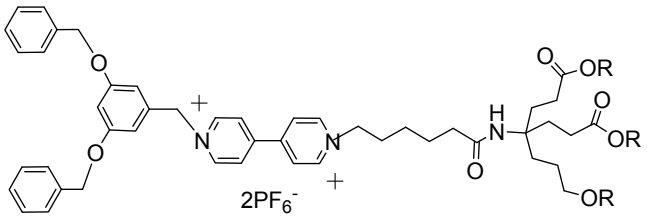

F1VN1E: R= *tert*-Butyl

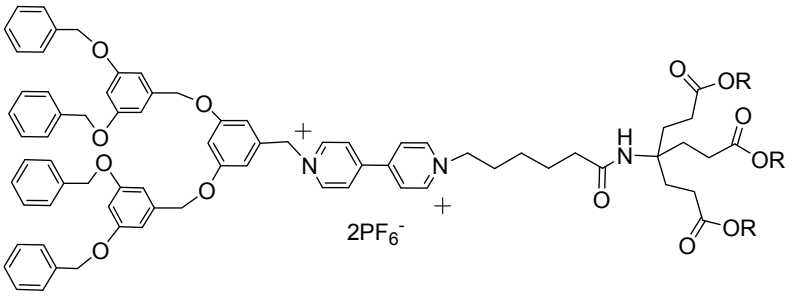

F2VN1E: R= *tert*-Butyl

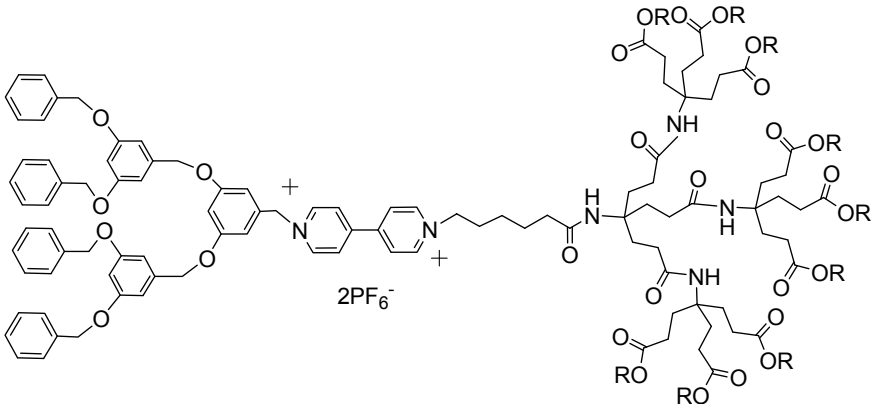

F2VN2E: R= *tert*-Butyl

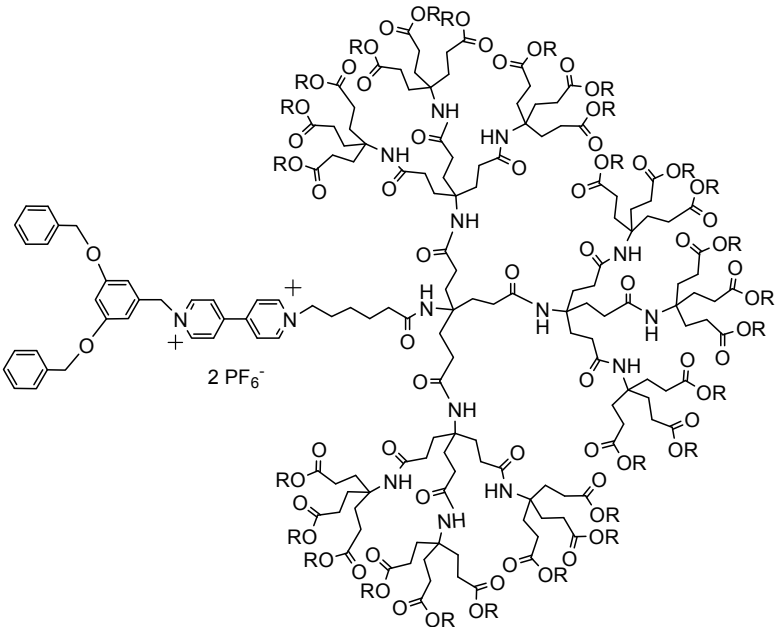

F1VN3E: R= *tert*-Butyl

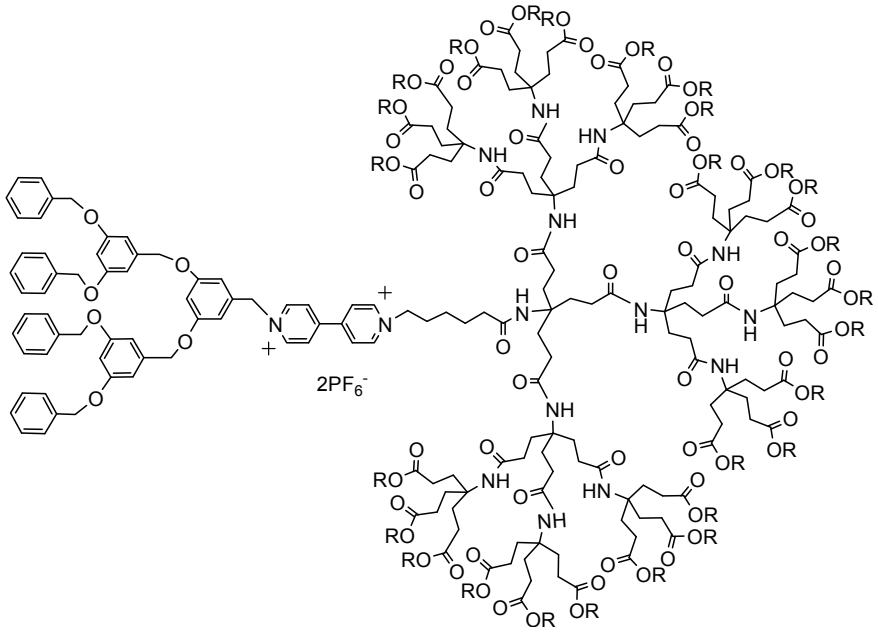

F2VN3E: R= *tert*-Butyl

Figure 2.6 *Structures of dendrimers synthesized. The naming system describes the building blocks present in each compound around the viologen core (V), F#, generation number of Fréchet dendron: N#E, ester terminated generation number of Newkome dendron.*

All new dendrimers synthesized for this work were characterized by ^{1}H, ^{13}C NMR spectroscopies and FAB or MALDI-TOF mass spectra.

These hybrid dendrimers could be considered as an excellent scaffold for structurally mimicking redox proteins. The structures with higher generations of Newkome and Fréchet dendrons, the viologen core is almost fully encapsulated.[24] The convergent synthetic strategy allows the synthesis of these molecules with excellent control in molecular weight. The amide linkage of the Newkome type dendrons also mimics structurally very closely the protein structure.

2.3 Electrochemistry of FVNE Dendrimers

The electrochemistry of viologen-containing dendrimers is governed by two one-electron reductions of the bipyridyl unit or popularly known viologen moiety. Viologen is very well known as an organic material to show reversible electrochemistry.[25] The first one-electron reduction generates a radical cation, which can be further reduced reversibly to a neutral species.

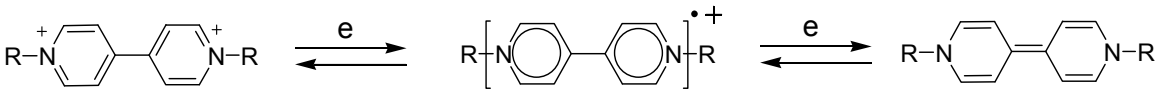

Dication Cation radical Neutral

The primary interest of my current work is to investigate the effect of the three dimensional dendritic microenvironment on the reduction potential of the viologen group.

The half-wave potentials, $E_{1/2}^1$ and $\Delta E_{1/2}^2$, of the viologen core dendrimers were determined from their corresponding cyclic voltammograms (**Table 2.1**). For F2VN3E, the peak current was very low and Osteryoung square wave voltammetry (OSWV) was used, along with cyclic voltammetry, to get accurate potential values.

Table 2.1 *Half-wave potentials ($E_{1/2}^1$ and $E_{1/2}^2$, in mV vs Ag/AgCl) for viologen-containing dendrimers at 25 °C in several organic solvents also containing 0.1 M $TBAPF_6$ as the supporting electrolyte.*

Solvent		F1VN1E	F2VN1E	F2VN2E	F1VN3E	F2VN3E
DCM	$E_{1/2}^1$	-240	-240	-277	-351	-292
	$E_{1/2}^2$	-755	-764	-772	-821	-784
THF	$E_{1/2}^1$	-276	-271	-285	-320	-300
	$E_{1/2}^2$	-676	-670	-685	-706	-708
ACN	$E_{1/2}^1$	-325	-322	-345	-369	-358
	$E_{1/2}^2$	-754	-756	-770	-776	-772

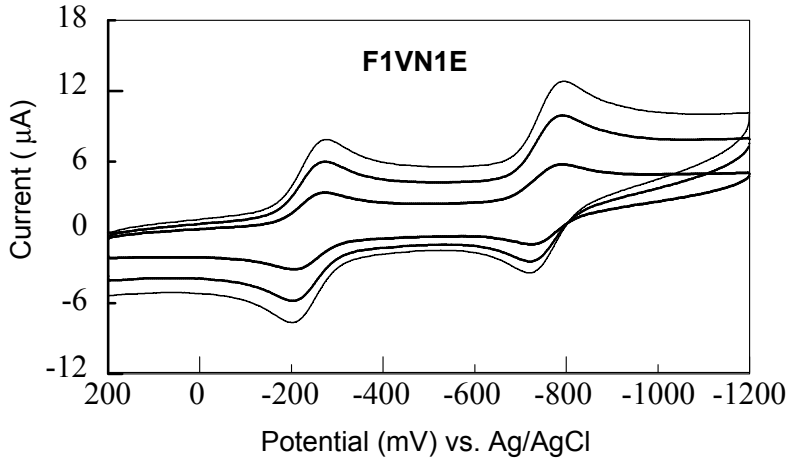
F1VN1E
Current (μA)
18
12
6
0
-6
-12
200
0
-200
-400
-600
-800
-1000
-1200
Potential (mV) vs. Ag/AgCl

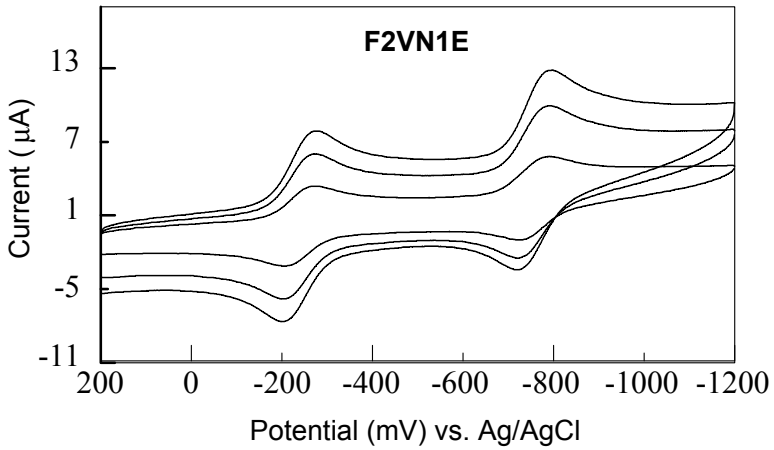
F2VN1E
Current (μA)
13
7
1
-5
-11
200
0
-200
-400
-600
-800
-1000
-1200
Potential (mV) vs. Ag/AgCl

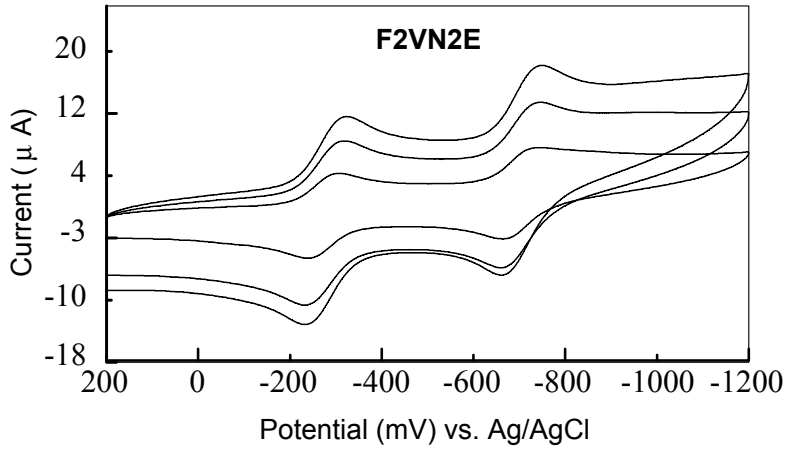
F2VN2E
Current (μ A)
20
12
4
-3
-10
-18
200
0
-200
-400
-600
-800
-1000
-1200
Potential (mV) vs. Ag/AgCl

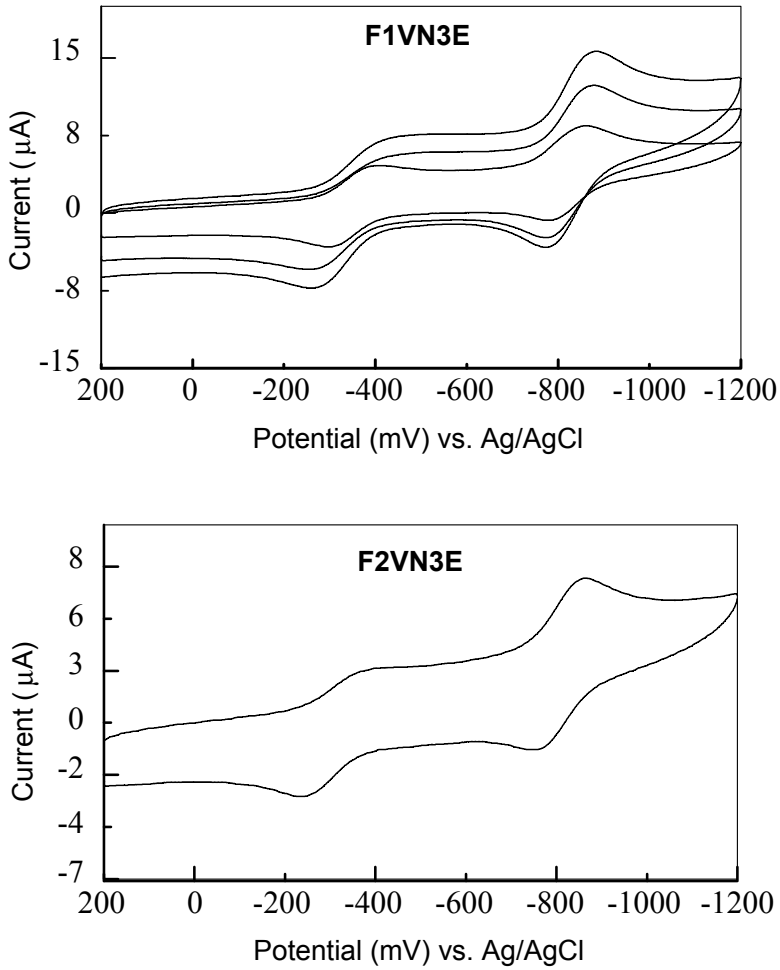

Figure 2.7 *Cyclic voltammetric response on a glassy carbon electrode (0.071 cm^2) of a 0.5 mM solution of F1VN1E, F2VN1E, F2VN2E, F1VN3E and F2VN3E dendrimer in dichloromethane also containing 0.1 M $TBAPF_6$. The current-potential curves shown were recorded at scan rates 0.1, 0.3 and 0.5 V/s, except the scan rate of F2VN3E was 0.1 V/s.*

The trend of half wave potentials ($E_{1/2}$) of these viologen core dendrimers varies according to the attached dendron. In relatively less polar solvents such as dichloromethane (DCM), the Newkome dendron, characterized by the presence of amide groups, provides a polar microenvironment for the viologen core with increasing generation number. This polar microenvironment thermodynamically stabilizes the positive charge on the viologen unit. In other words, it becomes

more difficult to remove the positive charge from the viologen as the generation number of the dendrimer increases. On the other hand, Fréchet dendron has aromatic ether linkage as the functional group, which is hydrophobic in nature. It would help the removal of the positive charge and thus has the reverse effect on $E_{1/2}$. However, from previous studies of our group, we know that the effect of Fréchet dendron on $E_{1/2}$ is not very pronounced compared to the Newkome dendron. The reason lies in their structural differences. Newkome dendrons are AB_3 type and surround the core three dimensionally in a very compact fashion. On the other hand, Fréchet dendrons grow as AB_2 and due to the planar phenyl groups, it forms wedges and tends to expand out away from the core.

The nature and effectiveness of Fréchet and Newkome dendrons on the half-wave potentials were clearly demonstrated by the $E_{1/2}$ values of the FVNE dendrimers. For example, in DCM, if we vary the Newkome dendron from 1st to 3rd generation while keeping the Fréchet dendron fixed (F1VN1E to F1VN3E), there is a -111 mV difference in the first reduction potential. On the other hand, if we keep the Newkome dendrons fixed and vary the Fréchet dendron from 1st generation to 2nd generation (F1VN1E to F2VN1E), $E_{1/2}{}^{1}$ increases only 5 mV and 3 mV in THF and ACN solution respectively. This indicates that Newkome dendron has more pronounced and reverse effect on the half-wave potentials when compared to the Fréchet dendron. This trend is very consistent throughout the dendrimer series. For example, the change for the first reduction going from F2VN1E to F2VN2E is -33mV and from F2VN1E to F2VN3E, this value is -52 mV. Again, this shows the buffering effect of the 2nd generation Fréchet dendron

which decreases the potential shift caused by the growth of the Newkome dendron. This trend was observed in THF as well as in acetonitrile.

The trend in the $E_{1/2}$ values may also be affected by the bulkiness of higher generation of Fréchet dendron. The Fréchet dendron is close to the core and probably sterically hinders the Newkome dendron to surround the core effectively. Thus the effect of Newkome dendron is weakened in the presence of a reasonably bulky Fréchet dendron.

We also analyzed the peak-to-peak splittings (ΔE_p in mV) of these dendrimer series. The values are summarized below (**Table 2.2**).

Table 2.2 *Molecular weights (MW), diffusion coefficients (D_0 x 10^6 cm^2/s), peak-to-peak splittings (ΔE_p^1 and ΔE_p^2, mV) and standard rate constants (10^3 k_o^1 and 10^3 k_o^2, cm s^{-1}) in 1:1 (ACN: DCM) at 25° C for the two one-electron reductions of the viologen-containing dendrimers of Figure 2.7. ΔE_p values were measured with 0.1 M $TBAPF_6$ as supporting electrolyte while the D_o values were measured without $TBAPF_6$.*

	F1VN1E	F2VN1E	F2VN2E	F1VN3E	F2VN3E
MW	1262	1671	2711	5359	5784
D_o	7.78	6.84	6.02	4.16	4.19
ΔE_p^1	61	66	68	81	na*
ΔE_p^2	63	62	65	65	107
k_o^1	Fast	3.68	2.59	0.95	na*
k_o^2	Fast	12.4	11.5	3.58	0.36

**na values are not available due to very flat nature of the voltammogram*

The lower generation dendrimers exhibit fast heterogeneous electron transfer

process. For higher generation dendrimers e.g., F2VN2E, F2VN3E, F1VN3E, ΔE_p is in the quasi-reversible range. This was anticipated based on our group's previous knowledge of reversible electrochemistry of viologen dendrimers. For faster scan rates, ΔE_p values increase. The heterogeneous electron transfer rate was calculated from Nicholson's method.[26] For the larger dendrimers F1VN3E and F2VN3E, the viologen core is almost encapsulated and we observe a slower rate of heterogeneous electron transfer.

The diffusion coefficient (D_o) was measured using PGSE NMR technique. According to the Stokes-Einstein equation (**Equation 1**), for spherical molecules moving in a continuous medium, the diffusion coefficient is inversely proportional to the effective hydrodynamic radius (r) of the diffusing species.

$$D_o = \frac{kT}{6\pi\eta r} \qquad \text{Equation 1}$$

Where k is the Boltzmann constant, T is the absolute temperature and η is the viscosity of the medium.

One of the preconditions of using equation 1 is it assumes the molecules as spherical in shape. However, the dendrimers synthesized in this work have a very distinctive structure, which can be compared to two branches of trees joined together linearly. One of them has a hemispherical three-dimensional structure while the other branch has structure that is more flat. Despite these structural differences, we see that the D_o for smaller dendrimers changes according to their molecular weight. In case of F1VN3E and F2VN3E, we observed a slight discrepancy.

2.4 Conclusion and Outlook

We prepared novel redox active hybrid dendrimers with unique structures. The reduction potentials of the viologen unit show a very reasonable trend as we grow the dendron from 1st to 3rd generation and combine Fréchet and Newkome dendrons in different possible ways.

These results are significant in light of the site encapsulation of redox proteins. The higher generation of these dendrimers, e.g. F2VN3E and F2VN1E, encapsulate the redox site with a high degree. The attenuation in heterogeneous electron transfer rate infers this kind of site encapsulation.

2.5 Experimental

2.5.1 Materials

Electrochemical grade tetrabutylammonium hexafluorophosphate (>99%) was purchased from Fluka (Milwaukee, WI) and used as received. Ammonium hexafluorophosphate was purchased from Aldrich (Milwaukee, WI). Ethyl acetate, methanol, nitromethane and methylene chloride were purchased from Fisher scientific (Suwanee, GA). EDC HCl (98+ %), DMF (<50ppm H_2O) and Al-Ni (50/50) alloy were purchased from Acros Organics (Somerville, NJ). O-(7-Azabenzotiazol-1-yl)-N, N, N', N'-tetramethyluronium hexafluorophosphate (N-HATU) (97%) was purchased from PE (Applied) Biosystems (Foster, CA). Acetonitrile-d_3 and methylene chloride-d_2 were obtained from Cambridge Isotope Laboratories (Andover, MA). Voltammetric experiments were performed using a Bioanalytical Systems (BAS, West Lafayette, IN) 100 B/W workstation controlled by a 200 MHz Pentium PC. Water was purified in a Barnstead NANOpure II system. Experiments were carried out using a glassy carbon working electrode, area ~0.07cm^2, platinum wire counter electrode and Ag/AgCl reference electrode from CH Instruments (Austin, TX). FAB-MS were obtained using a VG Trio 2000 (Manchester, UK). MALDI-TOF MS were obtained using a Bruker Biflex IV (Billerica, MA). ^1H, ^{13}C and PGSE NMR experiments were performed using a Bruker (Billerica, MA) Advance 400 MHz spectrometer with a GAB gradient unit capable of producing magnetic pulsed field gradients in the z-direction up to 0.5 Tm^{-1}.

2.5.2 Synthesis of Viologen Core (V) and Dendritic Building Blocks N1E, N2E, N3E and F1, F2, F2

The viologen core (V) was synthesized according to literature procedure.[21] Newkome type building blocks were synthesized according to literature procedure.[22] Fréchet type building blocks were synthesized according to published procedures.[7]

2.5.3 General Procedure for the Synthesis of FVNE

Viologen acid containing Fréchet dendron, F1V (400 mg, 0.463 mmol), Behera's amine N1E (213.64 mg, 0.514 mmol), *n*- HATU (195,18, 0.514 mmol) and 1,8-Bis (dimethylamino) naphthalene, N, N, N, N-tetramethyl-1, 8-naphthalenediamine (Proton Sponge, 110.24 mg, 0.514 mmol) were stirred in 3 mL of dry DMF for 12 h under N_2. The solution was concentrated under vacuum, diluted with 20 mL of EtOAc, and then extracted with 1 M NH_4Cl (2 x 10 mL) and brine (2 x 10 mL). The organic layer was concentrated and loaded into a chromatographic column (SiO_2). The chromatographic column was first eluted with EtOAc and then with 60:40 (acetone) / (7:2:1 (MeOH: 2 M NH_4Cl:CH_3NO_2)). The organic solvents on the combined fractions were removed under vacuum. After evaporation of the solvents, acetone was added to the oily residue, and then a saturated solution of NH_4PF_6 in 2:1 acetone: H_2O was added. The solution was stirred for 30 min further before acetone was gently removed under vacuum. The remaining oily suspension was extracted with EtOAc (2 x 10 mL). The combined extracts were dried over anhydrous Na_2SO_4 and the organic solvent was evaporated and chased with CH_2Cl_2 to afford the viologen

dendrimer as pale yellow solid. The final product was purified by washing with hexanes and dried under vacuum overnight to get ~ 80 mg of F1VN1E.

Yield: 13.7 %

The same procedure was used for F2VN1E, F2VN2E, F2VN3E and F1VN3E (with the appropriate building blocks second generation and third generation analogue of Behera's amine and Fréchet dendron). F1VN1E and F2VN1E were highly hydroscopic; F2VN2E was moderately hydroscopic while F1VN3E and F2VN3E were slightly hydroscopic. Yield for all these dendrimers were 10-14 %.

F1VN1E: ^{1}H NMR (400 MHz, CD_3CN): 1.38 (27H, s), 1.6 (2H, m), 1.85 (6H, t), 2.05 (4H,m), 2.1 (8H, t), 4.64 (2H, t), 5.09 (4H, s), 5.70 (2H, s), 5.91 (1H, s), 6.71 (3H, ds), 7.3-7.4 (10H, m), 8.4 (4H, d), 8.9 (4H, dd). ^{13}C NMR (100 MHz, CD_3CN): 25.40, 26.18, 28.65, 30.58, 30.65, 31.83, 36.97, 58.55, 61.36, 63.06, 65.97, 71.42, 81.28, 104.38, 109.83, 128.61, 128.74, 129.11, 129.98, 136.10, 138.12, 146.94, 162.06, 172.12, 173.53, 174.02. FAB-MS: m/z 972 $[M-2PF_6]^+$

F2VN1E: ^{1}H NMR (400 MHz, CD_2Cl_2): 1.39 (27H, s), 1.44 (2H, m), 1.59 (2H, m), 1.84 (6H, t), 2.05 (2H, m), 2.16 (8H, t), 4.37 (2H, t), 4.9-4.94 (12H, ds), 5.46 (2H, s), 5.88 (1H, s), 6.5 (2H, s), 6.59-6.63 (7H, ds), 7.22-7.36 (20H, m), 8.2 (4H, d), 8.8 (4H, dd). ^{13}C NMR (100 MHz, CD_2Cl_2): 28.4, 30.75, 31.14, 71.22, 81.71, 103.1, 107.5, 128.56, 128.8, 129.07, 129.21, 138.61, 147.22, 162.1, 162.5, 174.15. FAB-MS: m/z 1542 $[M-PF_6]^+$,1396 $[M-2PF_6]^+$

F2VN2E: ^{1}H NMR (400 MHz, CD_3CN): 1.39 (81H, s), 1.6 (4H, m), 1.82 (28H, t), 2.1 (26H, t), 4.67 (2H, t), 5.04-5.09 (12H, ds), 5.71 (2H, s), 6.03 (4H, s), 6.57 (4H, s), 6.65 (3H, s), 6.68 (2H, s), 7.32-7.41 (20 H, m), 8.41 (4H, d), 8.99 (4H, dd). ^{13}C

NMR (100 MHz, CD_3CN): 24.68, 25.72, 28.77, 30.75, 32.32, 32.40, 58.57, 59.05, 71.17, 71.22, 81.34, 102.86, 108.04, 109.91, 109.99, 128.68, 128.82, 129.09, 129.16, 129.40, 129.55, 129.96, 130.03, 136.13, 138.56, 161.53, 161.94, 173.60, 174.01. MALDI-TOF: m/z 2565 $[M\text{-}PF_6]^+$, 2420 $[M\text{-}2PF_6]^+$

F1VN3E: ^1H NMR (400 MHz, CD_2Cl_2): 1.41 (243H, s), 1.91 (84H, m), 2.14 (80H, t), 4.74 (2H, t), 5.05 (4H, s), 5.81 (2H, s), 6.68 (1H, s) 6.74 (2H, d), 7.39 (10H, m), 8.62 (4H, t), 9.07 (4H, t). ^{13}C NMR (100 MHz, CD_2Cl_2): 24.35, 28.36, 30.31, 30.38, 31.38, 31.62, 31.69, 58.31, 58.35, 68.53, 70.85, 81.41, 81.47, 108.94, 128.22, 128.68, 129.13, 129.29, 129.53, 137.03, 145.98, 146.14, 173.85, 173.93, 174.40, 174.62. MALDI-TOF: m/z 5071 $[M\text{-}2PF_6]^+$

F2VN3E: ^1H NMR (400 MHz, CD_2Cl_2): 1.41 (243H, s), 1.90 (84H, t), 2.14 (80H, t), 4.68 (2H, t), 5.00 (4H, s), 5.02 (8H, s), 5.78 (2H, s), 6.55 (3H, t), 6.66 (6H, ds), 7.31-7.41 (20H, m), 8.50 (4H, m), 8.94-8.99 (4H, m). ^{13}C NMR (100 MHz, CD_2Cl_2): 23.60, 24.40, 28.41, 29.60, 30.36, 31.00, 32.56, 39.42, 58.46, 68.64, 70.68, 81.66, 102.14, 107.05, 128.22, 128.60, 128.78, 129.14, 129.35, 129.59, 131.52, 137.57, 139.57, 160.78, 161.52, 168.20, 174.17, 174.91, 175.07. MALDI-TOF: m/z 5498 $[M\text{-}2PF_6]^+$.

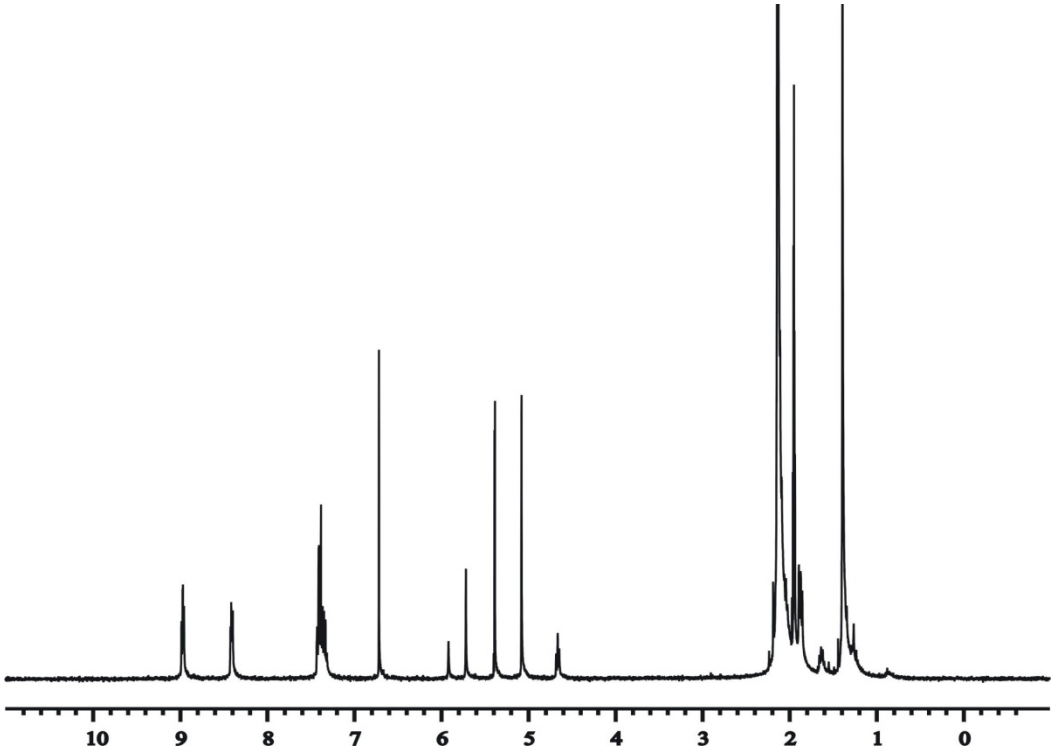

Spectra 2.1 *^{1}H NMR Spectra of F1VN1E in CD_3CN*

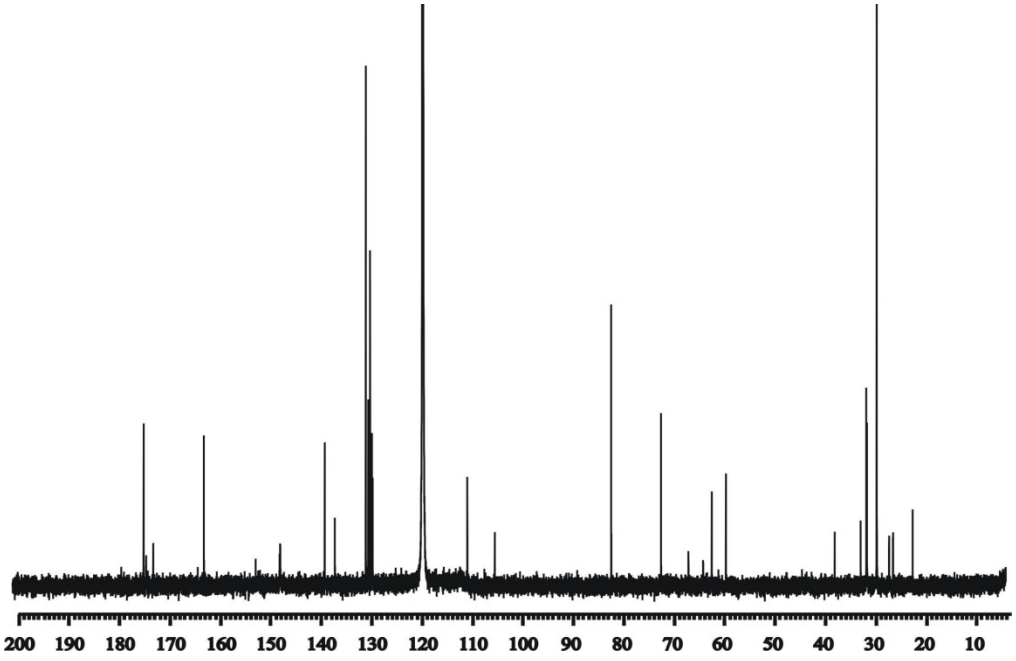

Spectra 2.2 *^{13}C NMR spectra of FIVN1E in CD_3CN*

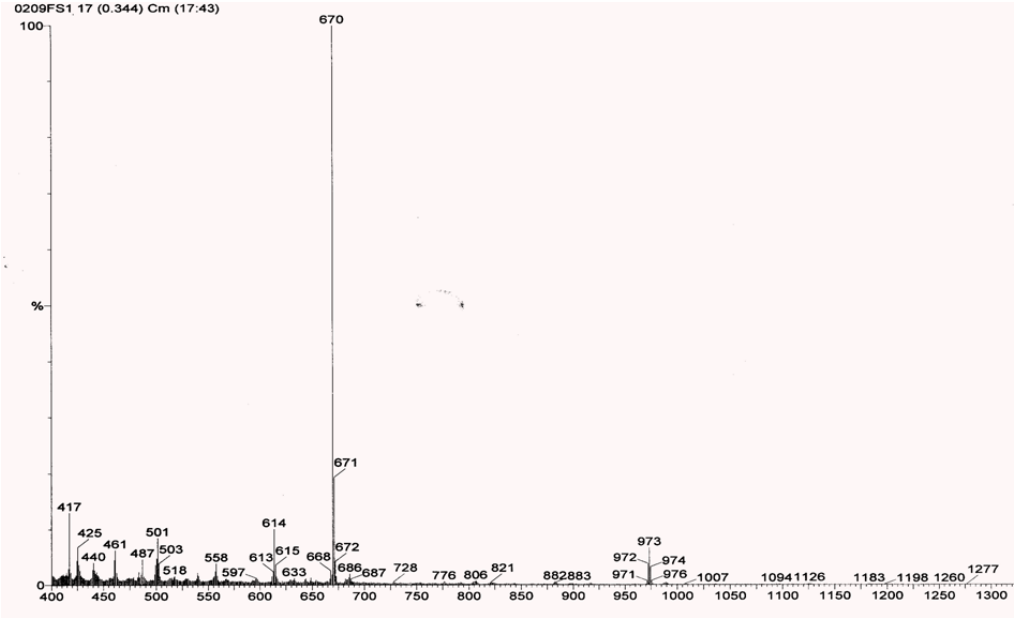

Spectra 2.3 *FAB-MS spectra of F1VN1E*

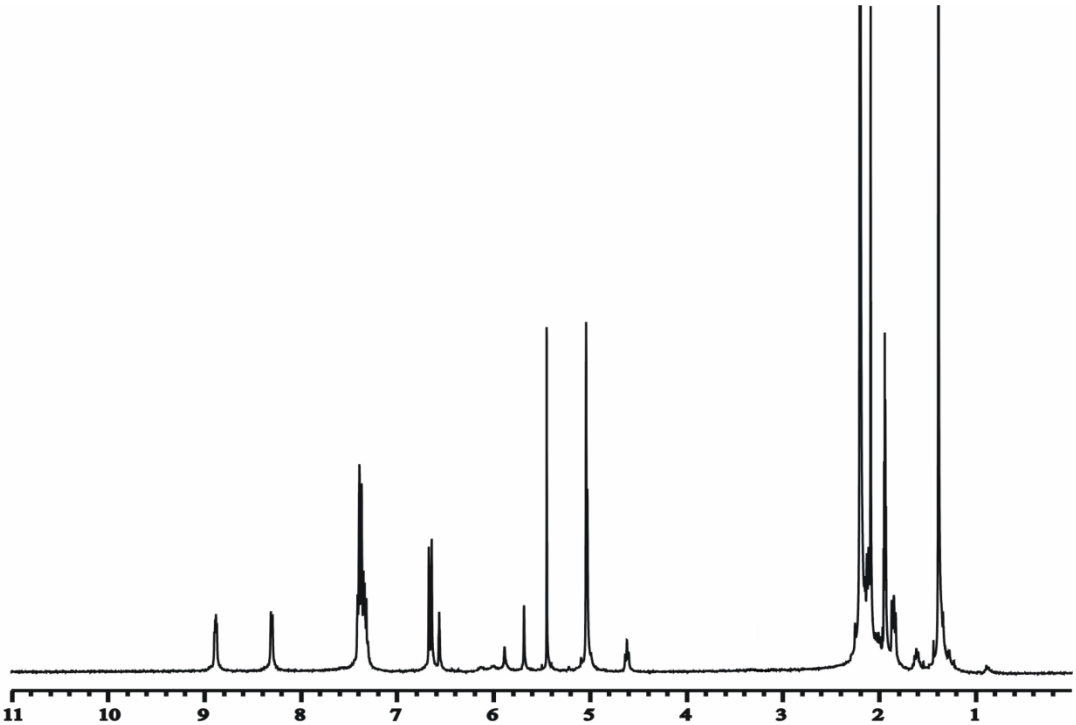

Spectra 2.4 *^{1}H NMR spectra of F2VN1E in CD_2Cl_2*

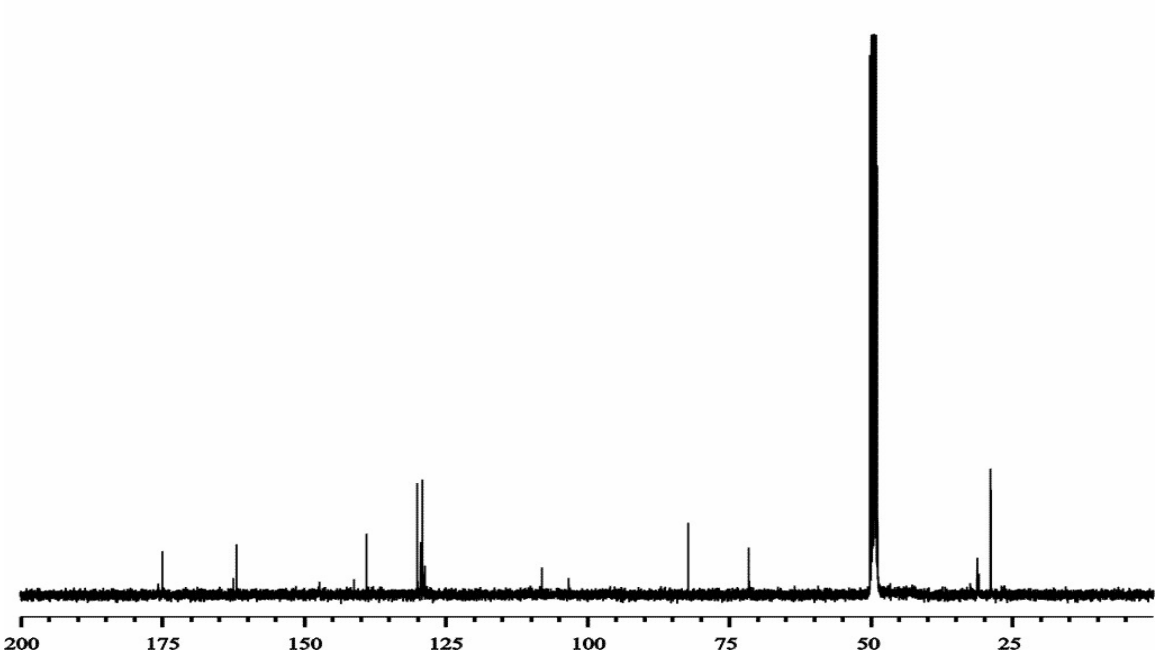

Spectra 2.5 *^{13}C NMR spectra of F2VN1E in CD_2Cl_2*

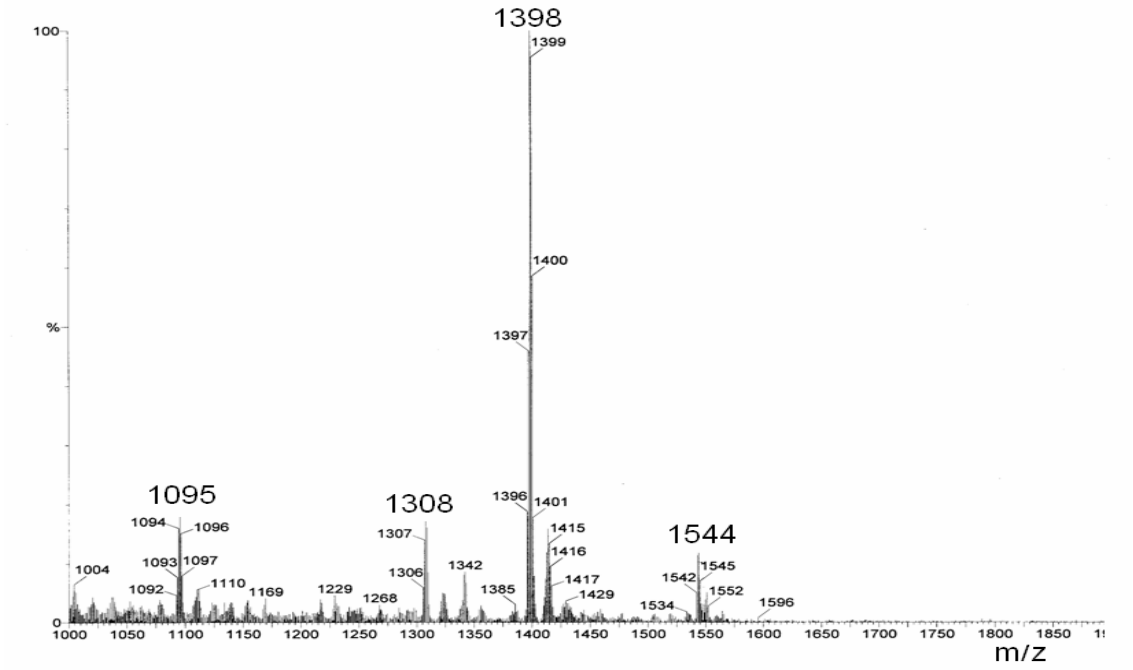

Spectra 2.6 *FAB-MS spectra of F2VN1E*

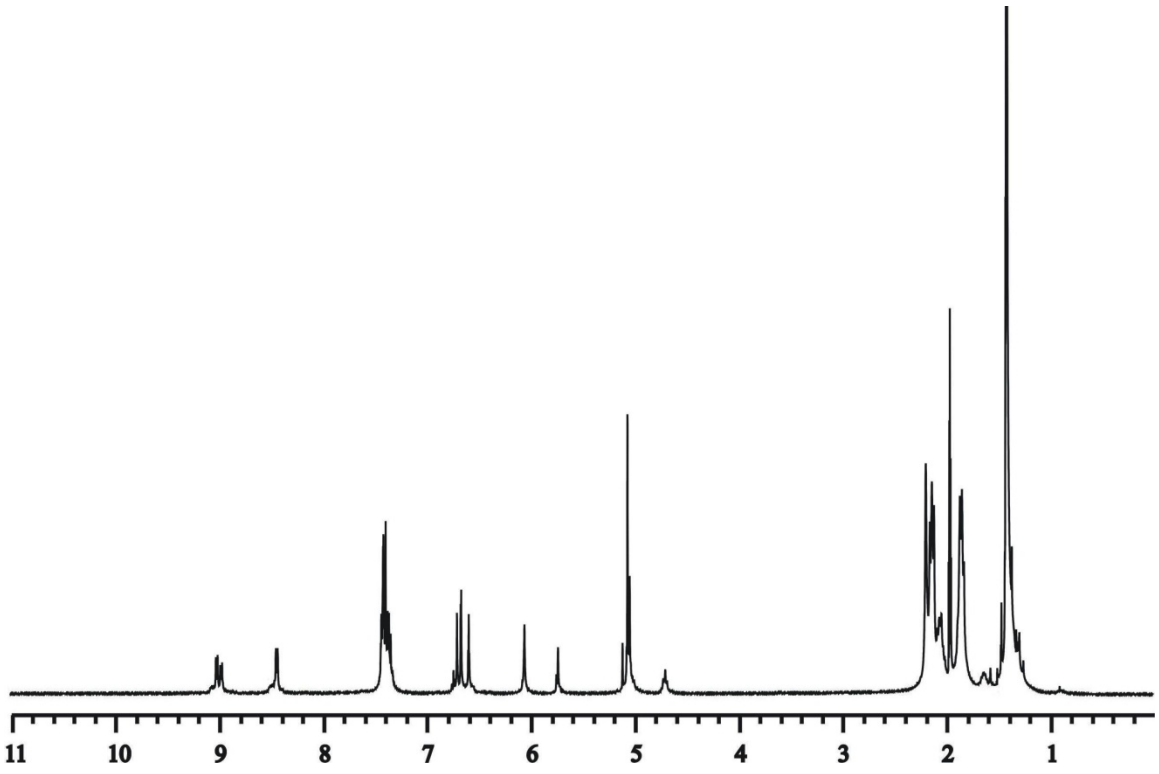

Spectra 2.7 *^{1}H NMR spectra of F2VN2E in CD3CN*

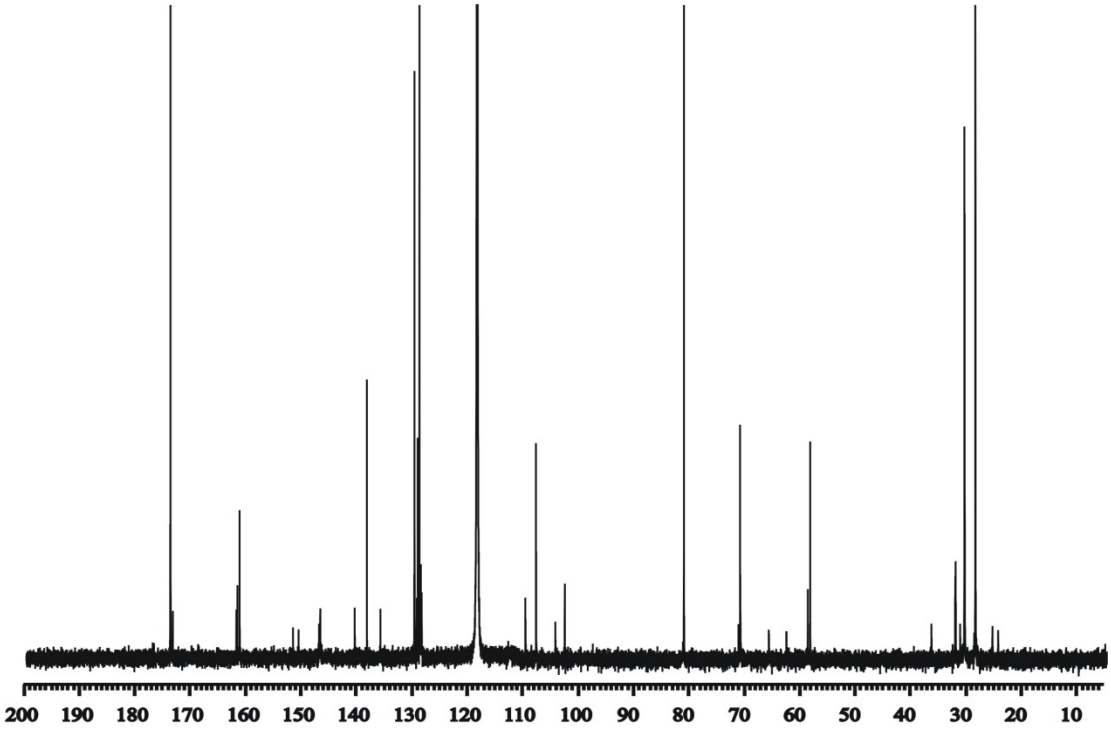

Spectra 2.8 *^{13}C NMR Spectra of F2N2 in CD_3CN*

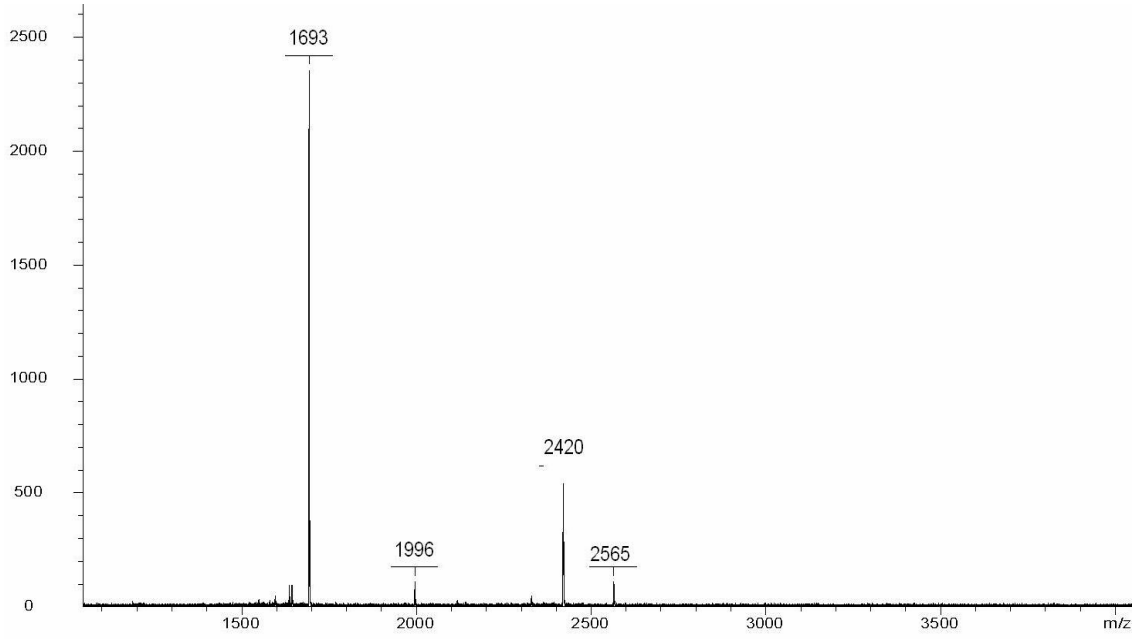

Spectra 2.9 *MALDI-TOF spectra of F2VN2E*

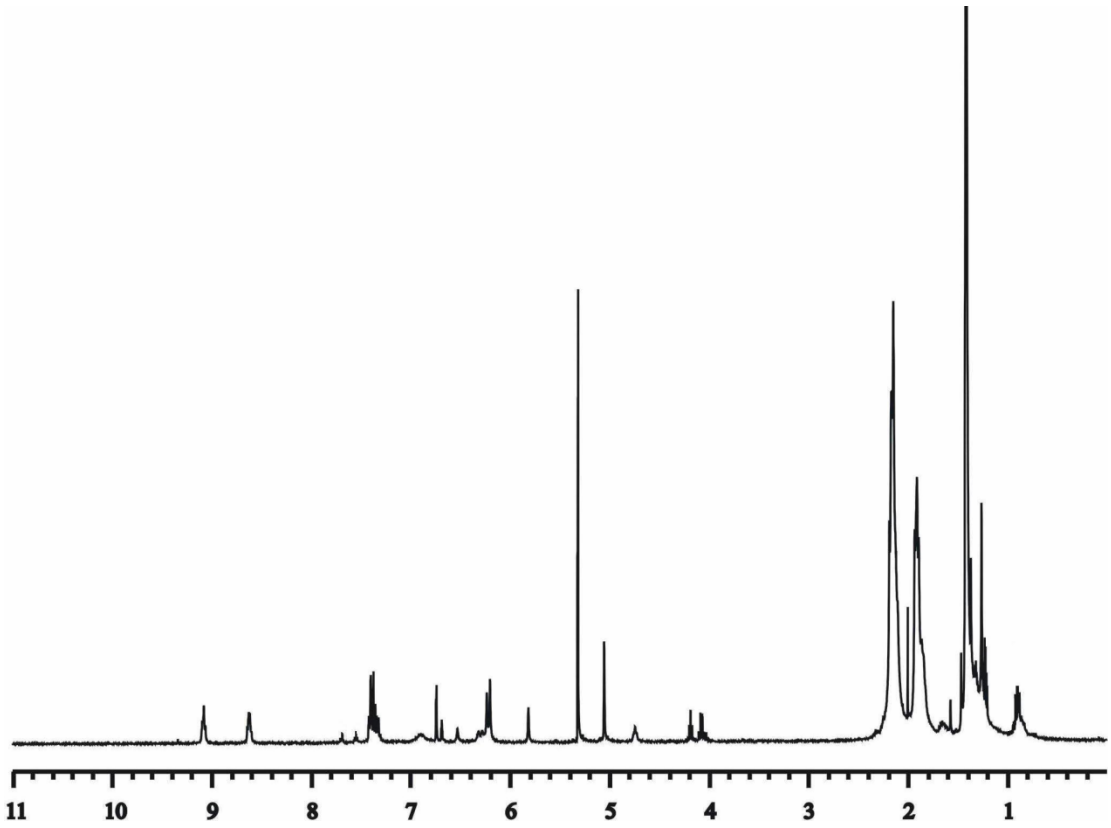

Spectra 2.10 *^{1}H NMR spectra of F1VN3E in CD_2Cl_2*

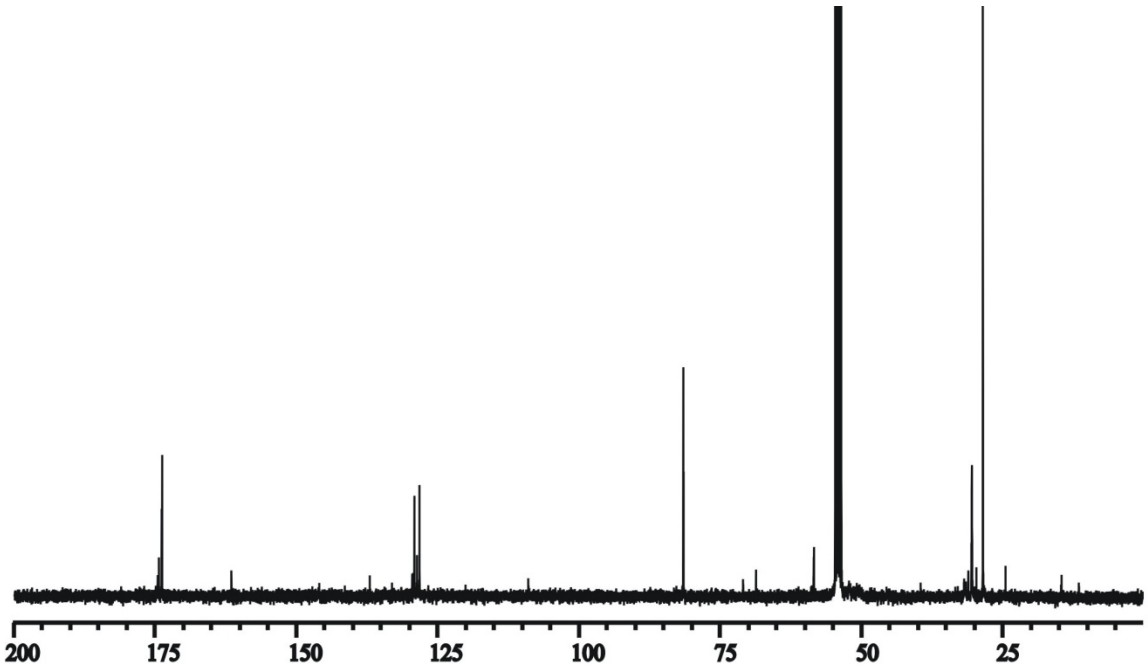

Spectra 2.11 *^{13}C NMR spectra of F1VN3E in CD_2Cl_2*

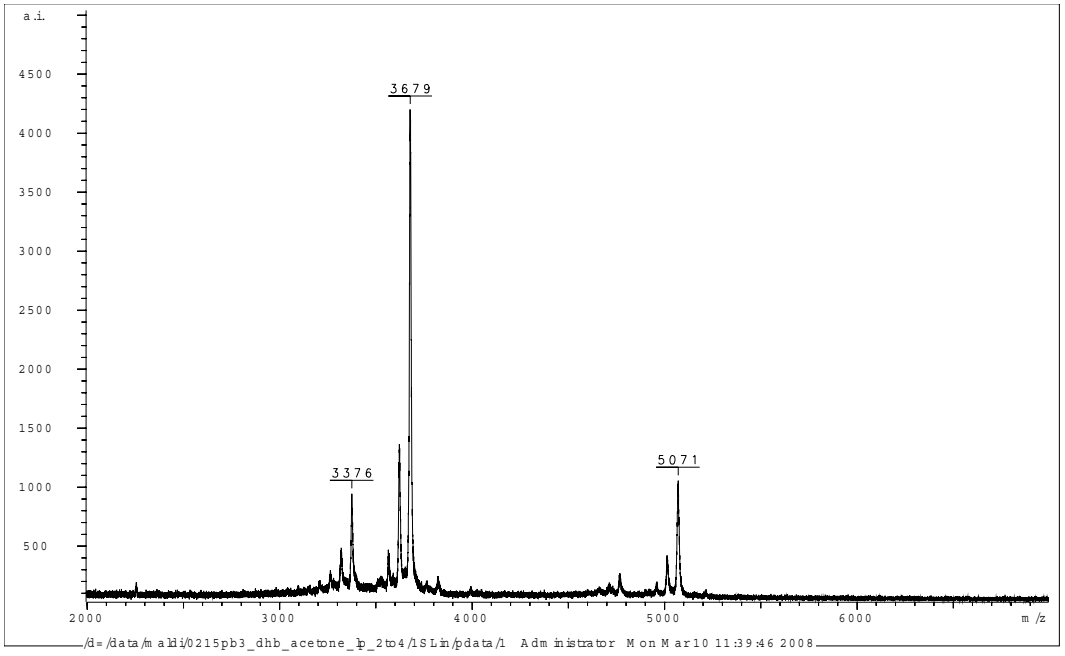

Spectra 2.12 *Mass spectra of F1VN3E*

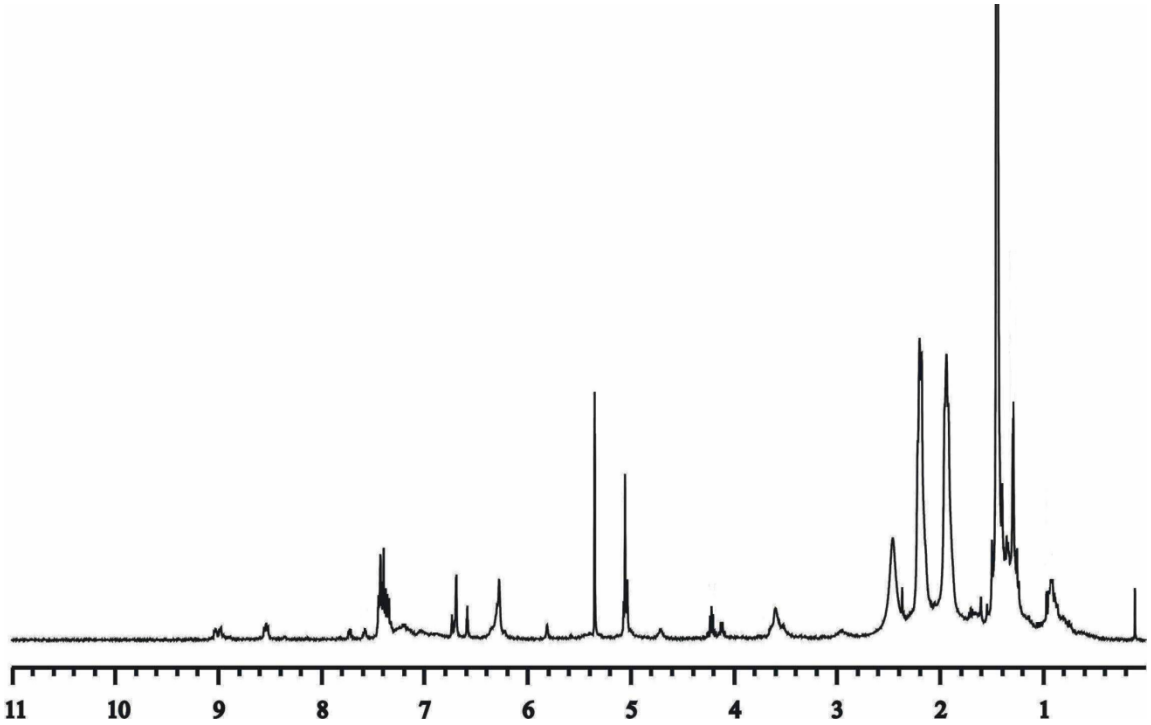

Spectra 2.13 *^{1}H NMR spectra of F2VN3E in CD_2Cl_2*

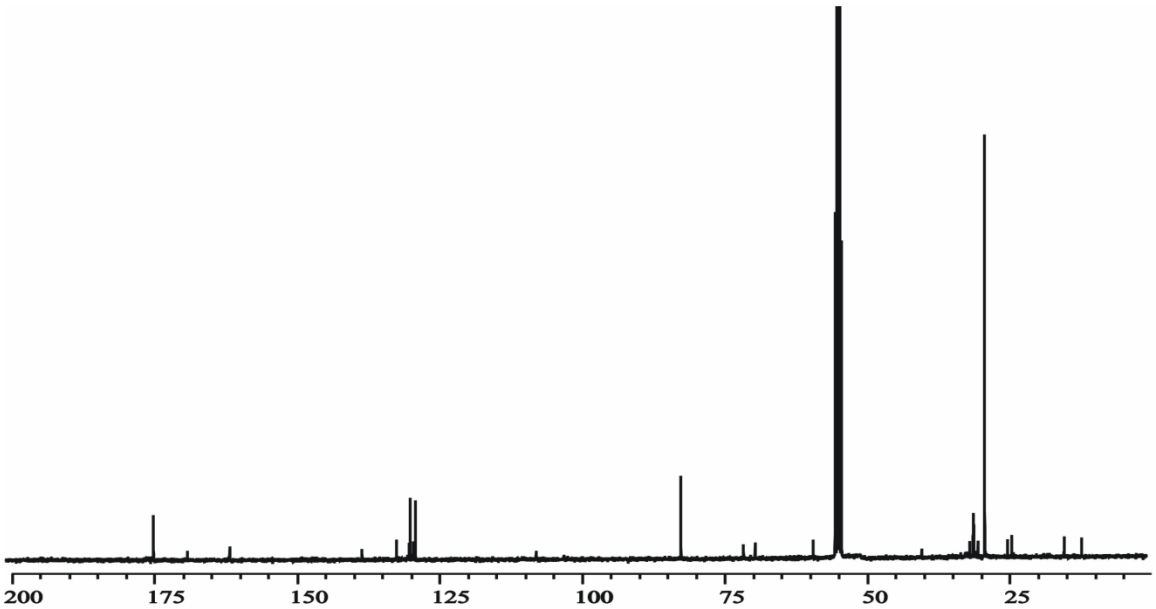

Spectra 2.14 *^{13}C NMR spectra of F2VN3E in CD_2Cl_2*

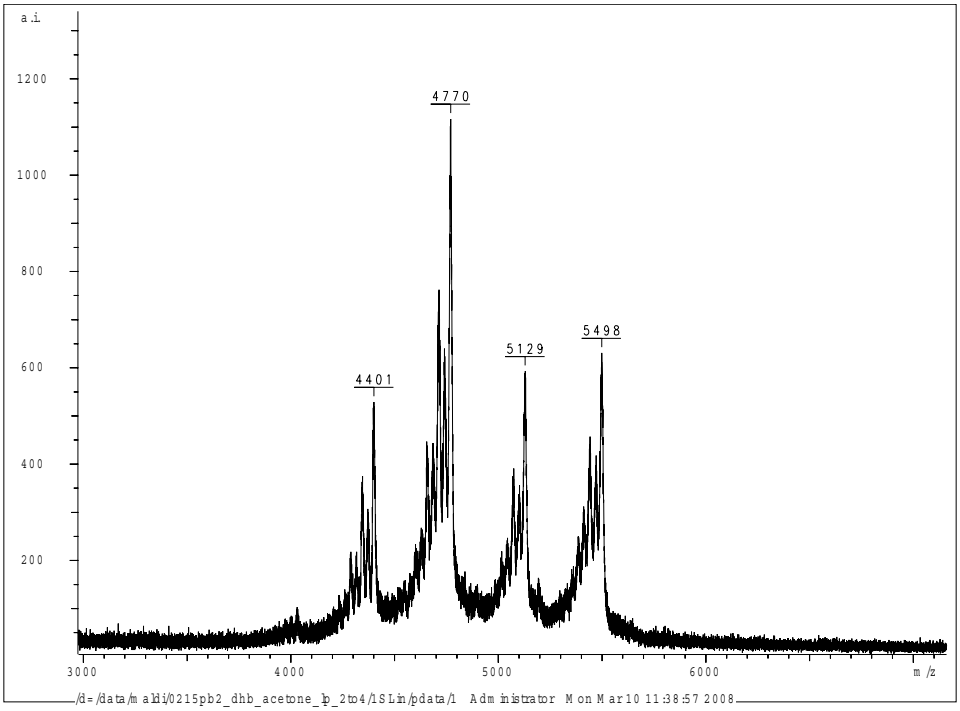

Spectra 2.15 *MALDI-TOF spectra of F2VN3E*

Chapter III

INVESTIGATION OF RESORCINARENE-TEMPO INCLUSION COMPLEX

3.1 Supramolecular Chemistry of Resorcinarene

3.1.1 Resorcinarene

Resorcinarenes are one of the very popular hosts in supramolecular chemistry. They can be easily synthesized by condensing resorcinol with aliphatic or aromatic aldehydes in the presence of acid. The first crystal structure of resorcinarene was determined by Erdtman and coworkers by single crystal x-ray analysis in 1968.[27] The hydroxyl groups on the upper rim of resorcinarene are capable to form multiple hydrogen bond. The four aromatic rings make the inner part of resorcinarene to be electron rich.

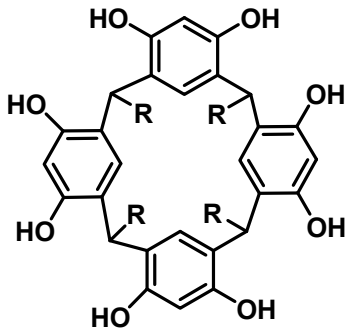

Figure 3.1 *General structure of resorcin[4]arene*

3.1.2 Hexameric Resorcinarene

Hydrogen-bonding is considered as one of the weakest forces in nature and yet multiple hydrogen bonds can make some of the most efficient binding especially where there is a need of dynamic binding. Some of the relevant

examples include DNA base pairing, protein folding in protein alpha helices, enzymatic binding to a substrate, etc.[28]

In 1997, McGillivray and Atwood reported the solid state crystal structure of the hexameric assembly of resorcinarenes.[29] The eight hydroxyl groups on the upper rim of resorcinarene are capable of hydrogen bonds. Six of the resorcinarene molecules together with eight water molecules are held very tightly by sixty –OH···O hydrogen bonds to form a molecular container. This molecular container is a very good host for many neutral molecules as well as cationic molecules. The main binding interactions for this kind of host-guest system are mainly hydrogen bonding, cation-π interaction.

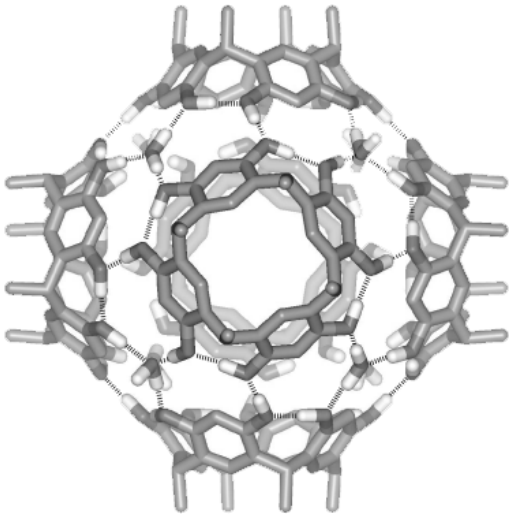

Figure 3.2 *Hexameric structure of resorcinarene*[29]

3.1.3 Resorcinarenes As Supramolecular Host

Resorcinarene has been employed as a host in monomeric as well as in hexameric form in supramolecular chemistry. Aoyama *et al.*[30] reported the host guest system of polar guest molecules of biological origin with monomeric

resorcinarene. The guest molecules have hydroxyl, amide or nitrogen heterocycles which can undergo favorable non-covalent interaction with the π-electron rich interior and can form hydrogen bonds with the hydroxyl groups of resorcinarene. They have also illustrated the resorcinarene complexes with sugar molecules with multiple hydrogen bonding. They also complexes with riboflavin (vitamin B_2) and cyanocobalamin (vitamin B_{12}).

The hexameric form of resorcinarene has a cavity size of 1375 $Å^3$ and is dynamic in nature. The capsule is very stable and can encapsulate a variety of guest with different sizes. Cohen and Rebek[31] have been actively working to find the nature and binding properties of these capsules.[31]

Shivanyuk and Rebek[32] studied the encapsulation of quaternary ammonium salts by resorcinarene in wet $CHCl_3$ solutions, varying the alkyl chain length from propyl to heptyl. The positively charged tetra-alkyl ammonium salts undergo encapsulation by favorable interaction of the positive charge and the π-electron rich interior of the capsule. The smaller ammonium salts share the cavity with a few solvent molecules. But as the size of alkyl chain length increases, there are less number of solvent molecules found inside the capsule. It's noteworthy that the longer alkyl chains, the heptyl and octyl chains undergo 'folding' to fit themselves within the cavity.

3.1.4 Encapsulation of Redox Active Probes Within Resorcinarene Cavity

Our group has explored the inclusion phenomenon of electroactive probes in hexameric resorcinarene. The guests used in this work were cobaltocenium ion and electrochemically generated ferrocenium ion.[33]

When ferrocene was used as a guest and electrochemically oxidized to ferrocenium ion in presence of the host, a new oxidation wave at more cathodic potentials appeared. This new wave grew until exactly 6 equivalents of resorcinarenes were added, indicating that the capsule is favoring the formation of the positive charge. Interestingly the reduction wave required an over potential of 500 mV indicating the high thermodynamic barrier to reduce back the ferrocenium cation to neutral ferrocene upon encapsulation. ^{1}H NMR experiments indicate there is no encapsulation with the neutral guest. The voltammetric experiments were performed in variety of supporting electrolytes. Surprisingly the tetralkyl ammonium salts used as supporting electrolyte did not interfere in this encapsulation process. However, if PF_6^-, BF_4^- and ClO_4^- were present as counter anion, this kind of complex formation was hindered.

3.2 EPR Study of Inclusion Phenomenon of Tempo and Resorcinarene

Previous studies showed that resorcinarene form nice hexameric capsules in solid state as well as in wet organic solvents.[34] These molecular capsules are good hosts for organic molecules especially for alkyl ammonium salts due to favorable cation-π interactions.

We probed the cavity of resorcinarene capsule with paramagnetic molecules. In general, host-guest interaction results certain changes in the environment surrounding the guest. For example, when tempo undergoes complexation with cucurbit[n]uril (CB) in aqueous media, polarity of the medium surrounding tempo changes from bulk water to a relatively hydrophobic cavity of CB.[35] In addition, the free rotation of uncomplexed tempo decreases to a large extent when it is confined within the CB cavity. EPR spectroscopy allows us to detect host-guest complexation when the radical used as guest shows an "environmental sensitivity", with a subsequent change of the spectroscopic parameters upon complexation.[36] In our present studies on inclusion phenomena of radicals species within the resorcinarene cavity, we used 4-amino-2, 2, 6, 6-tetramethylpiperidine-1-oxyl (or 4-amino tempo, G1) and 4-trimethyl- ammonium-2, 2, 6, 6-tetramethylpiperidine-1-oxyl, iodide (G2), and studied the complexation of these two guests by linearly varying the host concentration while the guest concentration is fixed.

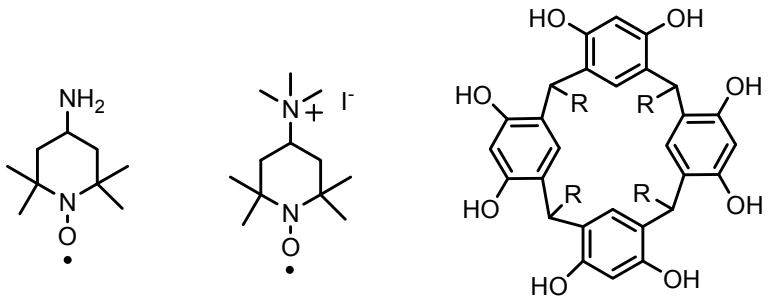

G1 G2 Resorcinarene
R: $(CH_2)_{10}CH_3$

Figure 3.3 *Structures of tempo (guest) and resorcinarene (host)*

EPR is a very powerful technique and complementary to NMR technique. The lifetime of EPR excitation is much shorter than NMR and is capable of giving a dynamic picture of the system.[37] The EPR spectra of 4-amino tempo (G1) as well as of 4-trimethyl ammonium tempo (G2) have three peaks due to the hyperfine coupling of the unpaired electron with the nitrogen nucleus. This is common for nitroxide radicals.

3.2.1 Results

The EPR study of the titration of these two guests produced interesting results. As we start adding resorcinarene, there was very little change in the spectra. But when 5-6 equivalents of the host was added, the spectra changed drastically, especially the high-field line broadened a lot.

The line broadening was much more significant when the guest had a positive charge (G2) compared to the neutral one (G1). This kind of line broadening is characteristic for tempo derivative when the molecular tumbling motion is being restricted.

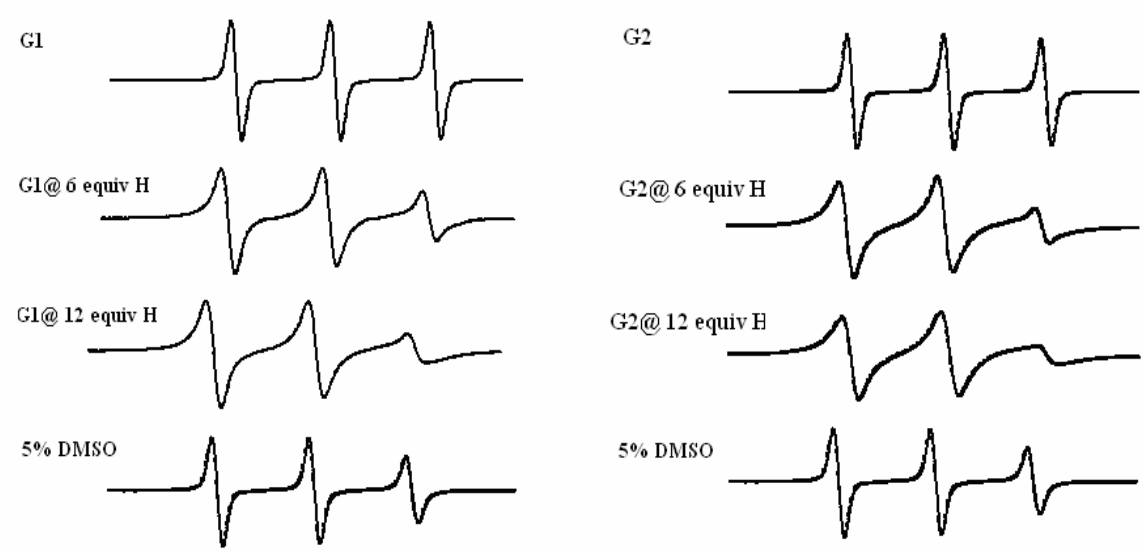

Figure 3.4 *EPR spectra of G1 and G2 with various amount of resorcinarene*

On addition of 5 % DMSO (v/v), the high-field line of the spectra changed back to sharp lines. This is probably because DMSO can break the hydrogen bonds responsible for resorcinarene capsule formation and the guest comes out of the capsule.

For further investigation of these inclusion phenomena in a more quantitative fashion, we calculated the rotational correlation time (RCT, τ). This is a useful tool for investigating the host-guest complexation in supramolecular chemistry. If a species has a longer rotational correlation time, it means it has some restriction to rotate freely around itself. On the other hand, a short τ indicates that the molecule has no restriction for rotation. Upon complexation, the free rotation of uncomplexed guest becomes restricted. This is reflected in the rotational correlation time of the guest.

We used this parameter to investigate the nature of tempo-resorcinarene system. The rotational correlation time at different stoichiometric ratios of host and guest were calculated using the following equation: [38]

$$\tau = 6.5 \times 10^{-10} \Delta H_0 \left[\sqrt{\frac{h_0}{h_{-1}}} + \sqrt{\frac{h_0}{h_{+1}}} - 2 \right] \qquad \text{Equation 2}$$

ΔH_0 is the peak-to-peak width (in Gauss) of the central line; h_{-1}, h_0 and h_1 are the heights of the low field, central, and the high field lines, respectively.

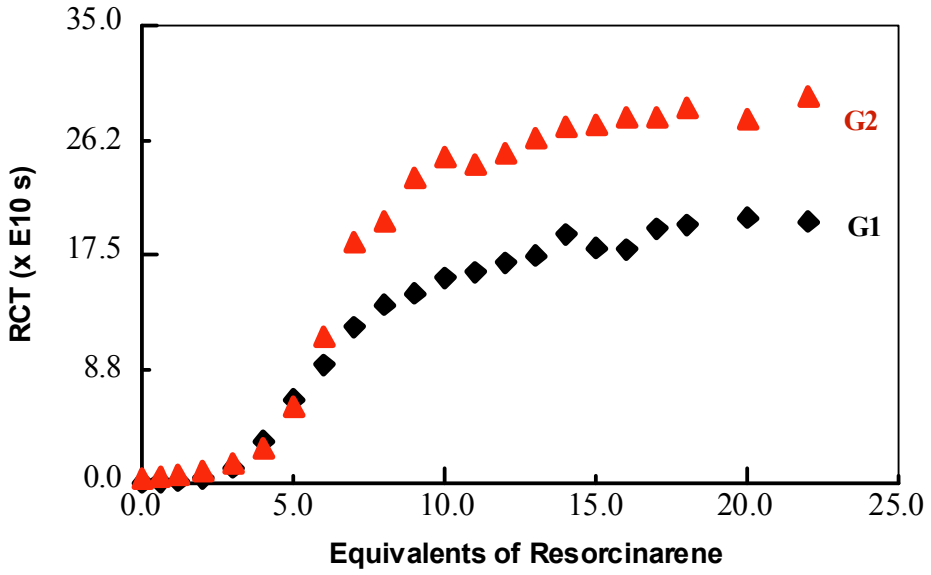

Figure 3.5 *Rotational correlation time of G1 and G2 plotted against the equivalents of resorcinarene.*

From the plot (**Figure 3.5**) we observe that the positively charged tempo (G2) slows down much more rapidly and to a larger extent upon encapsulation compared to the neutral one (G1). In addition, the rotational correlation time reached a saturation line after a certain amount of resorcinarene capsule was

present in the solution; G2 reached the saturation line slightly before G1. From these observations, we may conclude that G2 binds more strongly with these capsules than G1.

From our group's previous work on inclusion phenomenon of resorcinarene and cobaltocenium cation (Cob^+), we knew that these two species form a very stable complex. To compare the stability of tempo-resorcinarene vs. Cob^+-resorcinarene, we performed a competitive complexation titration. Cob^+ was added gradually to a solution of tempo and 1.5 capsules of resorcinarene (G @ 1.5 capsules) and the τ was calculated from the resulting EPR spectra (**Figure 3.6**).

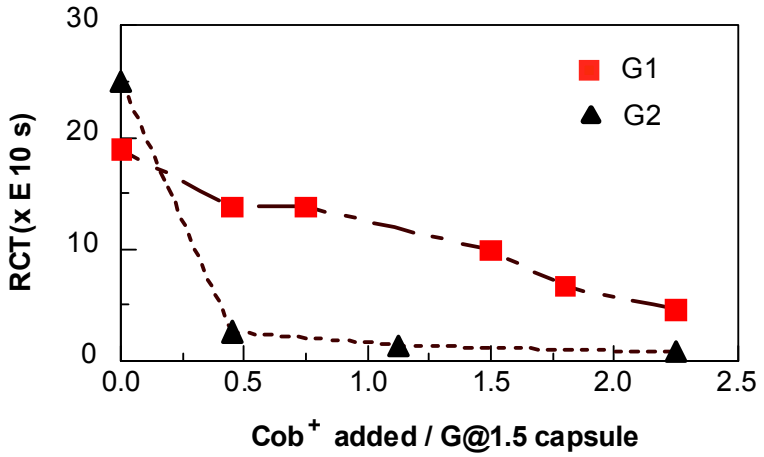

Figure 3.6 *Change in rotational correlation time (RCT) when Cob+ was added to G@ 1.5 resorcinarene capsule*

It was observed that Cob^+ replaces G2 completely with a huge decrease in rotational correlation time. In the case of G1, on addition of Cob^+, τ deceases significantly, but there is still some weak interactions remaining between G1 and resorcinarene. The amine function group of G1 is probably able to make H-bonds

3.3 NMR Study

We investigated the inclusion behavior by ^{1}H NMR to further confirm the results obtained from the EPR study. Tempo, being a paramagnetic substance, broadens the ^{1}H NMR signals of nearby protons of the host. We took advantage of this fact and titrated resorcinarene (3 mM) with varying amount (0-1mM) of G1 and G2. Upon inclusion the protons of resorcinarene cavity, that are very close to tempo, started to disappear. The ^{1}H NMR line widths at half-height (LW) was calculated and plotted against the equivalents of tempo added to a fixed amount of host (**Figure 3.7**).

In general, the LW does not change much at the beginning, but once 1 equivalent of guest was added per resorcinarene capsule, LW changed sharply and significantly. For G2, once there are ~1.5 guests per capsule the LW does not change much. This is probably due to the fact that the capsules are saturated with guest molecules.

In the case of G1, it requires more number of guests per host to complete the complexation indication a relatively lower binding constant. This is consistent with the EPR experiments where the host requires larger amount of guests to obtain In addition, the LW changes only after 1 equivalent of guest per capsule is present, but we could not go far to get the saturation line due to the high noise

in the NMR spectra. From these observations, we may conclude that G1 binds to resorcinarene with lower affinity to that of the G2.

.

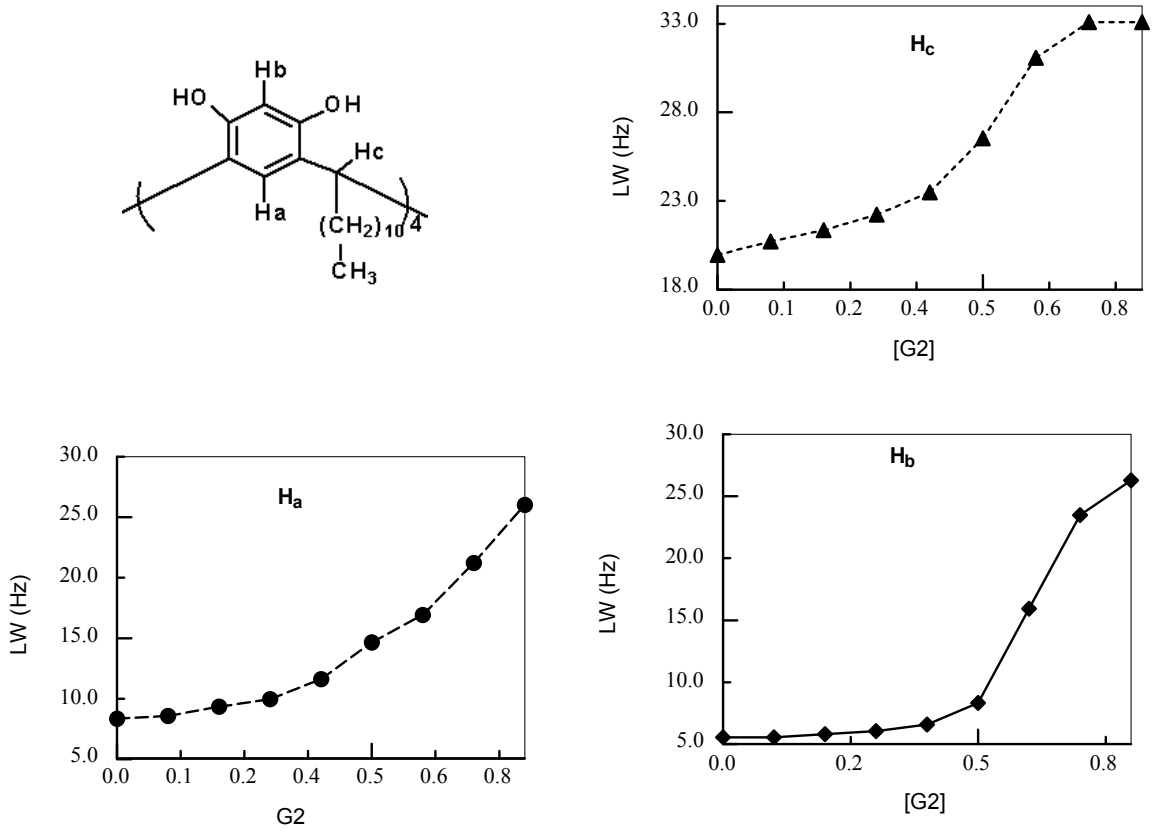

Figure 3.7 *^{1}H NMR line-width at half-height of the different protons of resorcinarene upon Inclusion with trimethyl ammonium tempo (G2)*

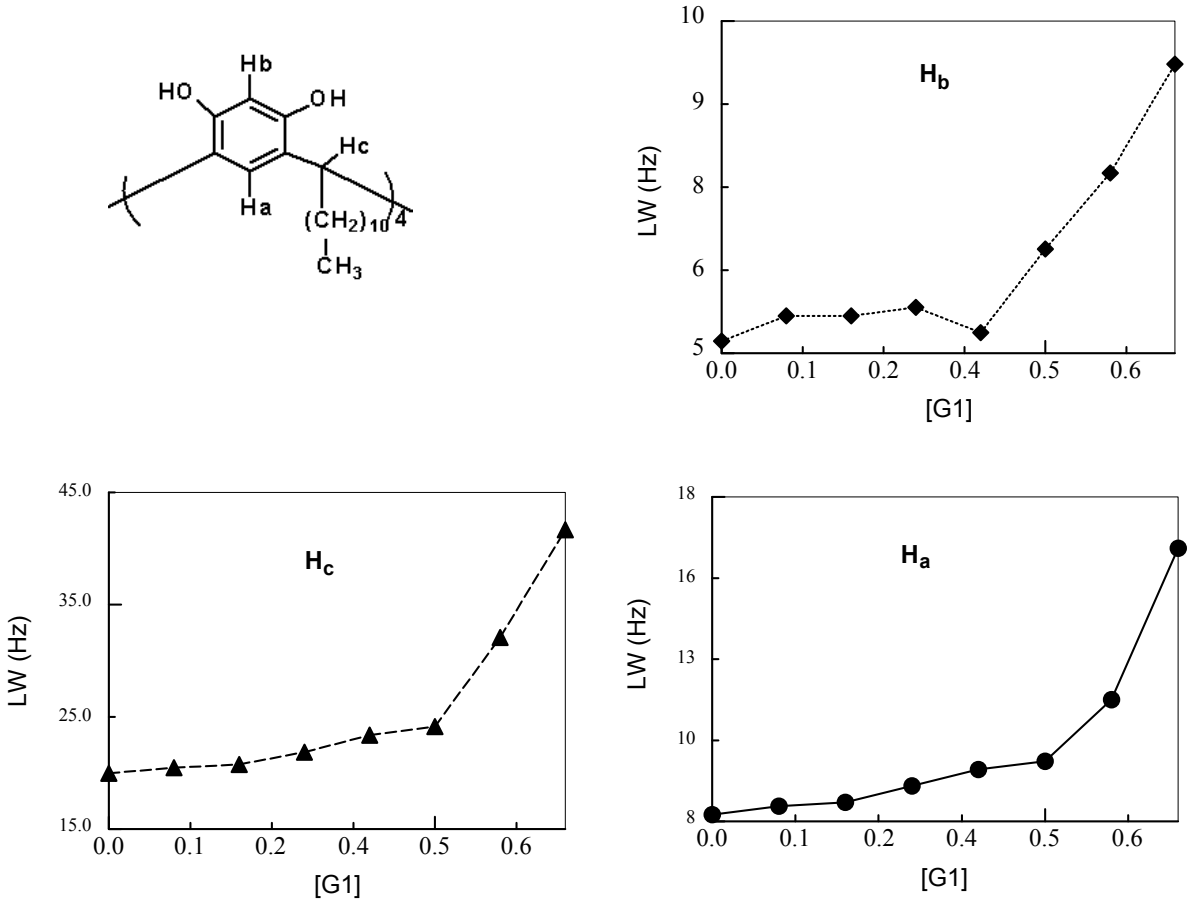

Figure 3.8 *^{1}H NMR line-width at half-height of the different protons of resorcinarene upon inclusion with 4-amino tempo (G1).*

We also investigated how the NMR peak of resorcinarene changes when we add tempo gradually. We observed that the peaks integrals of the protons near the cavity decreases gradually maintaining a nice curvature. This directly proves the interaction of the inner cavity protons and the tempo.

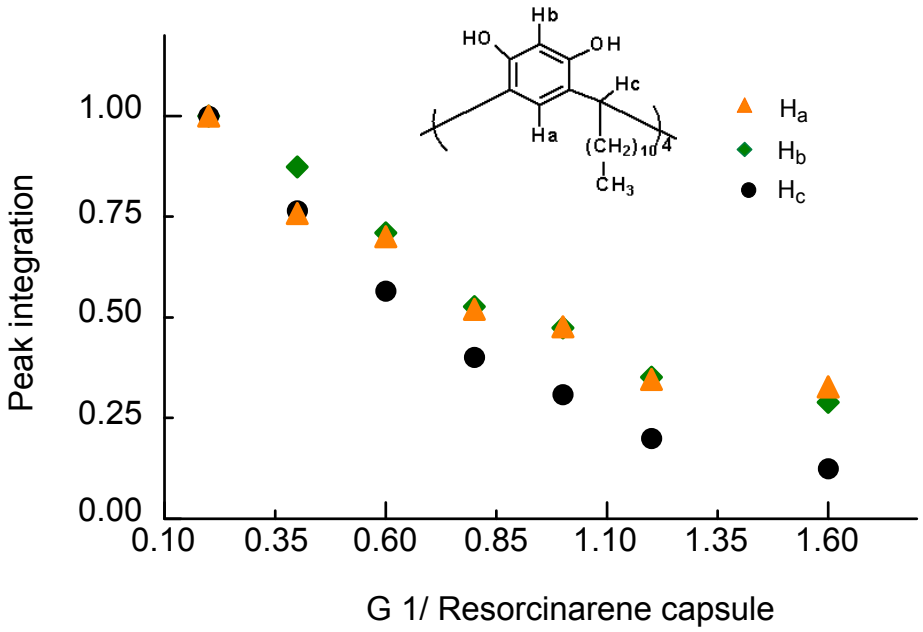

Figure 3.9 *Changes in NMR peak integrals on addition of G1*

3.4 Conclusion and Outlook

Cavity of resorcinarene capsule has been probed with paramagnetic guests. This work is significant because it showed, for the first time, the nature of the capsule in a very dynamic way.

From EPR as well as ^{1}H NMR we observed the evidence of complexation. The main non-covalent force acting in this inclusion phenomenon is hydrogen bonding for 4-amino tempo and hydrogen bonding as well as cation–π interaction for the 4-trimethyl ammonium tempo derivative. The positively charged tempo binds comparatively with higher affinity with the resorcinarene capsule than the neutral one. This investigation initiates the probing of resorcinarene capsules with radicals in a very different way.

3.5 Experimental

Resorcinarene was synthesized according to literature procedure.[39] 4-amino-2, 2, 6, 6-tetramethylpiperidine-1-oxyl (or 4-amino tempo) and 4-trimethyl-ammonium-2, 2, 6, 6-tetramethylpiperidine-1-oxyl, iodide were purchased from Aldrich (Milwaukee, WI). Methylene chloride was purchased from Fisher scientific and was stirred overnight with water to saturate it before use. Water was purified in a Barnstead NANOpure II system. Methylene chloride-d_2 was obtained from Cambridge Isotope Laboratories (Andover, MA). ^{1}H NMR experiments were performed using a Bruker (Billerica, MA) Advance 400 MHz spectrometer. EPR experiments were performed on a Bruker 200D EPR (Billerica, MA) spectrometer.

References

1 a) Archut, A.; Vogtle, F. *Chem. Soc. Rev*. **1998**, *27*, 233.
b) Zeng, F.; Zimmerman, S. C. *Chem. Rev.* **1997**, *97*, 1681.

2 a) Fischer, M.; Voegtle, F. *Angew. Chem., Int. Ed.* **1999***, 38*, 884.
b) Tomalia, D. A.; Dvornic, P. R. *Nature* **1994***, 372*, 617.
c) Knapen, J. W. J.; van der Made, A.W.; de Wilde, J. C., van Leeuwen, P. W. N. M.; Wijkens, P.; Grove, D. M.; van Koten, G. *Nature,* **1994***, 372*, 659.
d) Lee, C. L.; MacKay, J. A.; Fréchet, J. M. J.; Szoka, F. C. *Nature*, **2005**, *23*, 1517.

3) Buhleier, E.; Wehner, W.; Vögtle, F. *Synthesis* **1978**, 155.

4) Denkewalter, R.G.; Kolc, J.F.; Lukasavage, W. J.; U.S. Patent 4,410,688, **1983.**

5) Tomalia, D. A.; Naylo, A. M.; Goddard, W. *A. Angew. Chem.* **1990**, *102*,119.

6) Newkome, G. R.; Yao, Z.; G. R.; Gupta, V. K. *J. Org. Chem*. **1985**, *50*, 2003.

7) Wooley, K. L.; Hawker, A. J.; Fréchet, J. M. J. *J. Am. Chem. Soc*. **1981**, *113*, 4532.

8) De Brabander-van den Berg, E. M. M.; Meijer, E. W. *Angew. Chem.* **1993**, 105, 1370.

9) Xu, Z.; Moore, J. S. *Angew. Chem*. **1993**, *105*, 1394.

10) Caminati, G.; Turro, N. J.; Tomalia, D. A.; *J. Am. Chem. Soc.* **1990***, 112*, 8515.

11) Fischer, M.; Vögtle, F. *Angew. Chem., Int. Ed.* **1999***, 38*, 884.

12) Matthews, O. A.; Shipway, A. N.; Stoddart, J. F*. Prog. Polym. Sci*. **1998**, 23, 1.

13) Hodge, P. *Nature* **1993***, 362*, 18.

14) Hawker, C. J.; Fréchet, J. M. J. *J. Am. Chem. Soc.* **1990***, 112*, 7638.

15) Balzani, V.; Ceroni, P.;Gertermann, S.; Kauffmann, P.; Gorka, M.; Vögtle, F. *Chem. Commun,* **2000**, 853.

16) Garber, S. B.; Kingsbury, J. S.; Gray, B. L.; Hoveyda, A. H. *J. Am. Chem. Soc*, **2000**, *122*, 8168.

17) N. Malik et al., U.S. patent 7,005,124, **2006**.

18) Kobayashi, H.; Sato, N.; Hiraga, A.; *Magn. Reson. Med.* **2001**, 45, 454.

19) Takada, K.; Díaz, J. D.; Abruña, H. D.; Cuadrado, I.; Casado, C.; Alonso, B.; Morán, M.; Losada, J**.** *J*. Am. Chem. Soc. **1997**, *119*, 10763.

20 a) Cardona, C. M.; Kaifer, A. E. *J. Am. Chem. Soc.* **1998**, *120*, 4023.
b) Cardona, C. M.; McCarley, T. D.; Kaifer, A. E. *J. Org. Chem.* **2000**, *65*, 1857.

21) Ong, W.; Grindstaff, J.; Sobransingh, D.; Toba, R.; Quintela, J. M.; Peinador, C.; Kaifer, A. E. *J. Am. Chem. Soc.* **2005,** *127,* 3353.

22) Newkome, G. R.; Behera, R. K.; Moorefield, C. N.; Baker, G. R. *J. Org.Chem*. **1991**, *56*, 7162.

23 a) Cameron, C. S.; Gorman, C. B. *Adv. Funct. Mater*. **2002**, *12*, 17.
b) Toba, R.; Quintela, J. M.; Peinador, C.; Roman, E.; Kaifer, A. E. *Chem. Commun*. **2001**, 857.
c) Vicinelli, V.; Maestri, M.; Balzani, V.; Muller, U.; Hahn, U.; Osswald, F.; Vogtle, F. *New. J. Chem.* **2001**, *25*, 989.

24) Cameron, C. S.; Gorman, C. B. *Adv. Funct. Mater*. **2000**, *12*, 17.

25) Kaifer, A. E.; Gómez-Kaifer, M. *Supramolecular Electrochemistry* , 1st ed.; Wiley-Vch, **1999.**

26) Bard, A. J.; Faulkner, L. R. *Electrochemical Methods*: *Fundamentals and Applications*, 2nd ed.; Wiley: New York, **2001**; Chapter 6.

27) Erdtman, H.; Hogberg, S.; Abramsson, S.; Nilson, B. *Tetrahedron Lett.* **1968,** 1679.

28) Prins. L. J.; Reinhoudt, D. N.; Timmerman, P . *Angew. Chem. Int. Ed*. **2001**, *40,* 2382.

29) McGillivray, L. R.; Atwood, J. L. *Nature.* **1997**, *389***,** 469.

30) Aoyama, Y.; Tanaka, Y.; Toi, H.; Ogoshi, H. *J. Am. Chem. Soc*. **1988**, *110*, 634.

31) Conn, M. M.; Rebek, J., Jr. *Chem. Rev.* **1997**, *97*, 1647.

32) Shivanyuk, A.; Rebek, J. Jr. *Proc. Natl. Acad. Sci*. USA, **2001**, *98*, 7662.

33) Philip, I. E.; Kaifer, A. E. *J. Am. Chem. Soc*. **2002**, *124*, 12678.

34 a) Avram, L.; Cohen, Y. *J. Am. Chem. Soc* **. 2002**, *124*, 15148.
b) Conn, M. M.; Rebek, J., Jr. *Chem. Rev.* **1997**, *97*, 1647.
c) Aoyama, Y.; Tanaka, Y.; Toi, Y. H. Ogoshi, H. *J. Am. Chem. Soc*. **1988**, *110*, 634.

35) Mezzina, E.; Cruciani, F.; Pedulli, G.F.; Lucarini, M. *Chem. Eur. J.* **2007**, *13*, 7223.

36 a) Dykes, G. M.; Smith, D. K.; Caragheorgheopol**,** A. *Org . Biomol. Chem*. **2004**, *2,* 922.
b) Kotake, Y.; Janzen E. G. *J. Am. Chem. Soc.* **1988,** *110,* 3699.
c) Franchi, P.; Lucarini, M.; Franco, P. G. *Angew. Chem. Int. Ed*. **2003**, 42, 1842.

37 a) Wertz, J. E.; Bolton, J. R.; *Electron Spin Resonance: Elementary Theory and Practical Applications*, 1st ed.; McGraw-Hill Book Co., New York, **1972.**
b) Gordy, W.; *Theory and Applications of ESR*, 1 st ed.; John Wiley and Sons, New York, **1980**.

38) Ionita, G.; Chechik, V. *Org. Biomol. Chem*. **2005**, *3,* 3096.

39) Tunstad, L. M.; Tucker, J. A.; Dalcanale, E.;Weiser, J.; Bryant, J. A.; Sherman, J. C.; Helgeson, R. C.; Knobler, C. B.; Cram, D. J. *J. Org. Chem.* **1989**, *54*, 1305.